7

Energy Harvesting Cognitive Radios

7.1 Introduction

7.1.1 Cognitive Radio

Cognitive radio (CR) was proposed in 2005 to deal with the "spectrum scarcity" problem (Haykin 2005). Since Marconi's first trans-Atlantic radio transmission, more and more radio systems have been deployed over the years. All of these systems require a frequency band in the radio spectrum for operation. However, the radio spectrum is a scarce resource. In particular, the portion of the radio spectrum that is suitable for existing wireless technologies is very limited, mainly from 30 MHz to 3 GHz. If the frequency is too high, the propagation distance will decrease dramatically due to blockage. If the frequency is too low, the bandwidth will not be large enough to meet the quality of service (QoS) requirement. As more and better wireless services are being deployed, this portion of the radio spectrum is becoming more and more crowded. This is the so-called "spectrum scarcity" problem.

On the other hand, various studies in different countries have reported that the radio spectrum is in fact seriously under-utilized, although it looks very crowded (Chen and Oh 2016a). For example, studies commissioned by the Federal Communications Commission (FCC) in the US and the Office of Communications in the UK revealed that the percentage of the radio spectrum that is being used at any time in any location is usually low, between 15% and 80% in most cases (FCC Spectrum Policy Task 2002; QinetiQ 2007). Even in the city center of London, the frequency bands occupied by some very popular radio systems are rarely in operation (QinetiQ 2007). This creates the "spectrum under-utilization" problem.

Thus, we have a serious dilemma of insufficient spectrum resource and inefficient spectrum usage at the same time. This dilemma is largely caused by the regulators' current practices that impose a fixed spectrum access policy. Under this policy, a wireless system will normally be assigned an exclusive part of the radio spectrum as a license for operation to avoid interference from other users. This part of the radio spectrum cannot be used by any other users for any other purposes. For example, a TV band cannot be used to transmit mobile signals, and vice versa. This policy was made decades ago when there were not so many radio systems and when technologies were not so advanced as to be able to handle interference. Such a policy is not sustainable and is outdated given the dramatic development of wireless communications systems and the associated advances in software and hardware in recent years.

Energy Harvesting Communications: Principles and Theories, First Edition. Yunfei Chen.

To solve the problems of both "spectrum scarcity" and "spectrum under-utilization", dynamic spectrum access can be employed. One promising solution to the "spectrum scarcity" problem is to improve the efficiency of current spectrum utilization by allowing unlicensed "non-interfering" access to the licensed bands. In 2004, the FCC issued a notice to propose "no-harm" use of the licensed TV broadcasting bands in the USA (FCC 2004), as most US families use either satellite TV or cable TV. In the UK, Ofcom also proposed to increase the percentage of market-based bands to 71.5%. Owners of the market-based bands are allowed to trade and lease their bands to whoever wants to re-use their bands to maximize the social benefit of the spectrum. These governmental actions represent a new shift in the spectrum management policy. CR is a technological enabler of this new dynamic access policy. Figure 7.1 shows how the CR systems can use the spatial and temporal opportunities for operation. If the spatial opportunities are explored, CR and the primary user (PU) can operate at the same time but are far away from each other to avoid interference. If the temporal opportunities are explored, CR and PU operate at different time slots but in the same geographical area.

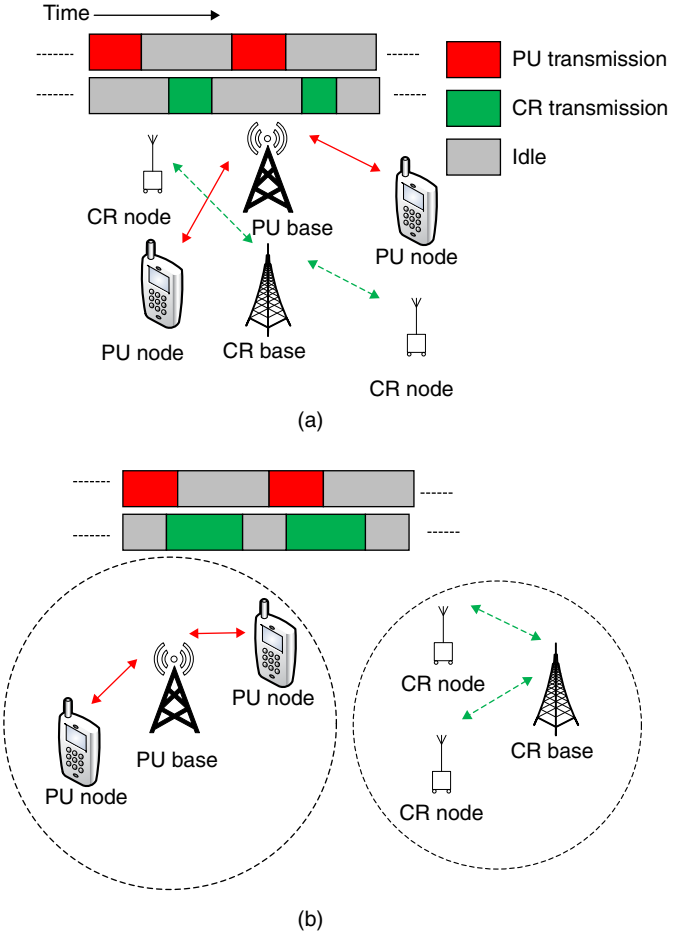

Figure 7.1 CR systems using (a) temporal and (b) spatial opportunities.

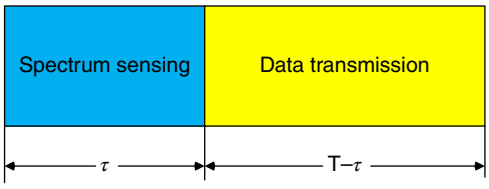

Figure 7.2 The frame structure of a conventional CR.

7.1.2 Cognitive Radio Functions

CR is a radio device that has cognition. The cognition is acquired by learning from and adapting to the radio environment during the operation. Therefore, CR is a radio-environment-aware device. To be more specific, CR first finds the parts of the radio spectrum that are not being occupied at some specific times in some specific locations, or the under-utilized spectrum, and then moves its operation to these parts called "spectrum holes" for opportunistic access, so that it does not need a fixed frequency band or license. Due to this attractive property, CR has already been adopted in several standardization works (Sherman et al. 2008).

In the physical layer, CR has two main functions: spectrum sensing; and data transmission. Spectrum sensing is probably more important than data transmission in the context of CR, as an inaccurate sensing will lead to interference with other systems, including the primary systems that own the license of the under-utilized spectrum, because they operate at the same frequency band in the radio spectrum. This will violate the non-interfering access rule. Consequently, it is of paramount importance to obtain spectrum sensing results as accurately as possible. Figure 7.2 shows the frame structure of a CR system with two main functions. When the total duration of the frame is fixed, there is a tradeoff between sensing and transmission (Liang et al. 2008).

7.1.3 Spectrum Sensing

The key function in CR is to find the empty frequency bands in the radio environment. This is accomplished by spectrum sensing.

Energy detection is probably one of the simplest methods for spectrum sensing (Urkowitz 1967). It measures the energy of the signal received from the interested band and compares this measurement with a predetermined threshold. The energy detector is very simple and easy to implement. However, it suffers from the noise uncertainty at a low signal-to-noise-ratio (SNR) (Tandra and Sahai 2008). This is caused by the error in the estimation of the noise power that is required in setting the detection threshold (Urkowitz 1967). Also, in a wireless environment with shadowing and/or fading, the random variation in the signal strength could reduce the SNR significantly and hence the energy detector may not be able to distinguish a heavily shadowed and/or faded signal from a zero signal very well. Consequently, it will think the channel is free to cause interference to the PU, the owner of the frequency band, who is actually operating.

To overcome this problem, feature-based detectors can be used. The feature-based detectors differentiate between signal and noise by using features of the signal, such as covariance and cyclostationarity, instead of the signal power (Chen et al. 2011b). They do not need the noise power in the detection threshold so they do not have the noise uncertainty problem. However, calculations of these features often require a large observation

interval and take a long time. Moreover, their performances deteriorate quickly in the presence of interference, as interference may have the same features as the signal. Thus, the feature-based detectors may be less desirable in applications where a quick detection decision is required or in applications where interference occurs.

To avoid long computation time as well as high computational cost, another method is to use energy detection in collaborative spectrum sensing (Chen and Beaulieu 2009). In collaborative spectrum sensing, energy measurements from several CR users are combined to reduce the noise uncertainty. Since collaborative spectrum sensing only involves linear or quadratic combination of the measurements, it provides simple, quick yet reliable detectors for spectrum sensing, even at a fairly low SNR. However, in order to perform collaboration, measurements have to be transmitted from the CR users to the fusion center through the CR links. This adds overheads to the CR network. Moreover, a strict network control has to be implemented to coordinate the transmission of measurements from all CR users.

7.1.4 Energy Harvesting Cognitive Radio

An energy harvesting CR is a radio device that has both cognition and energy harvesting capability. The cognition allows the unlicensed use of licensed frequency bands. Hence, it exploits the spectrum opportunities in the radio environment to help improve the spectral efficiency. On the other hand, energy harvesting is an important technology to achieve battery-free operations by replacing batteries with ambient energies from the surrounding environment. In particular, recent advances in electronics have made it possible to harvest the ambient electromagnetic waves in the radio environment for wireless communications, such as radio frequency identification and wireless body area networks. Thus, energy harvesting exploits the energy opportunities in the environment to save energy cost.

Two main costs of a wireless communications system are spectrum cost and energy cost. The spectrum cost can be considerably reduced by using CR with "free" bandwidth, while the energy cost can be significantly reduced by using energy harvesting with "free" energy. Thus, to provide a viable solution to reliable and sustainable wireless communications, it is imperative to design efficient energy harvesting CRs to reduce both spectrum and energy costs. For some applications, such as sensor networks, where a low-cost device is key to large-scale deployment, this will be very useful.

In the conventional CR, the main design constraint is collision avoidance. The CR needs to avoid collision with the PUs as much as possible, as it has lower priority on the use of the licensed band. This is often translated into a constraint on the transmission power, the transmission location, or the sensing period, etc. The conventional CR has two main functions: spectrum sensing; and data transmission. Hence, most design problems for the conventional CR involve the tradeoff between the accuracy of spectrum sensing and the throughput of data transmission, or the sensing-throughput tradeoff (Liang et al. 2008). The main design goal is to maximize the throughput or information rate subject to constraints on collision avoidance.

In the energy harvesting CR, the new feature of energy harvesting brings new challenges into CR designs. First, CR will have three functions to perform in the physical layer: spectrum sensing; data transmission; and energy harvesting. Thus, instead of the tradeoff between sensing and transmission, one has the tradeoff between

sensing, transmission, and harvesting. This makes the designs much more complicated. Secondly, in addition to the constraint on collision avoidance, there is an additional energy causality constraint. This constraint basically imposes a limitation that the energy must be harvested before it can be used for spectrum sensing or data transmission, or CR cannot use any future energy. In this case, unlike the conventional CR, the energy in the energy harvesting CR is dynamic and unstable. Hence, there is a possibility that the licensed channel is free but the CR user cannot use it due to insufficient energy. It is also possible that the licensed channel is busy but instead of remaining idle the CR user can harvest energy from the PU. The energy harvesting and spectrum sensing functions are performed at a receiver, while the data transmission function is performed at a transmitter. Their main design goals can be the maximization of throughput but can also be the maximization of the harvested energy subject to constraints on collision avoidance and energy causality.

Figure 7.3 compares the conventional CR with the energy harvesting CR in terms of their design problems. If the energy is harvested from the PU or the secondary

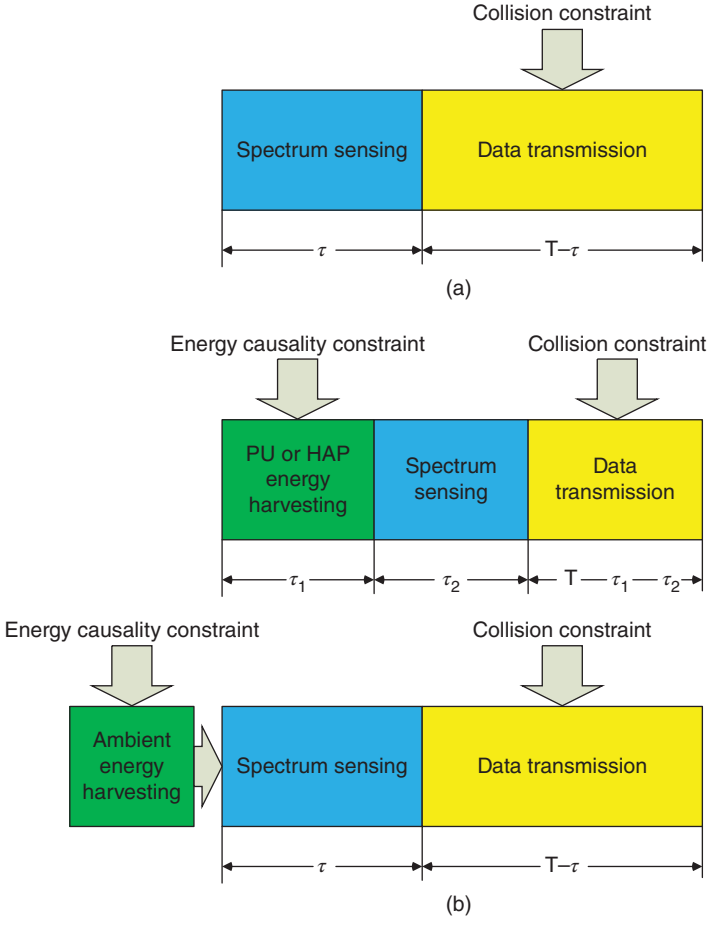

Figure 7.3 Comparison of (a) conventional CR and (b) energy harvesting CR.

base station, it requires extra energy harvesting time in the data packet. If the energy is harvested from the ambient sources, harvesting can be performed at the same time as sensing and transmission so that no extra harvesting time is required but the energy causality constraint still applies with greater uncertainty. Thus, most studies on energy harvesting CR focus on the tradeoff between sensing, transmission, and harvesting, subject to constraints on collision avoidance and energy causality. The collision avoidance is related to the dynamics of the PU traffic. The energy causality is related to the dynamics of the energy arrival process. If the CR harvests energy from the PU, the problem will be even more complicated, as the PU traffic and the harvested energy will be correlated.

Next, we will discuss several important technical challenges in energy harvesting CR. Before doing this, it is necessary to explain how the conventional CR and its spectrum sensing function work, as they are also part of the principles based on which energy harvesting CR works.

7.2 Conventional Cognitive Radio

7.2.1 Different Types of Cognitive Radio Systems

Depending on the spectrum sharing policies, there are three different types of CR systems: interweave; underlay; and overlay. They have different levels of cooperation between the CR and the PU and so their spectrum utilization efficiency also varies.

In the interweave CR system, the CR user is only allowed to access the licensed frequency band when the PU is not using it. This is also called opportunistic spectrum access. This policy imposes the strictest limitation on the CR user and provides the best protection for the PU. It is adopted in applications where the CR user and the PU do not have any interaction or cooperation. In this system, spectrum sensing is vital. It helps to find the "spectrum holes" in the spatial and temporal domains. Figure 7.1 actually gives the diagram of an interweave CR system, where the CR either operates at different time slots or different locations from the PU, depending on whether it exploits the temporal opportunities or spatial opportunities.

In the underlay CR system, the CR user is allowed to coexist with the PU, that is, the CR and the PU can operate in the same frequency band at the same time. From the PU's point of view, there is an increased level of noise floor caused by the CR that may affect its performance but this effect is negligible as long as the CR operates within the limit. This is very similar to the spread spectrum idea or the ultra-wide bandwidth technique. To protect the PU, there is an interference temperature imposed on the CR user. This interference temperature is essentially a constraint on the peak transmission power and the average transmission power of the CR, or a probability of power outage of the PU. Thus, in this case, although the CR can coexist with the PU, it must operate at a low transmission power. This requires a minimum level of cooperation or interaction between the CR and the PU. Figure 7.4 compares an underlay CR system with an interweave CR system, both of which utilize the spectrum holes in the time domain. Their main difference is how they behave when the PU is detected. In interweave CR, it stops transmission when the PU is detected, while in underlay CR, it reduces its transmission power when the PU is detected.

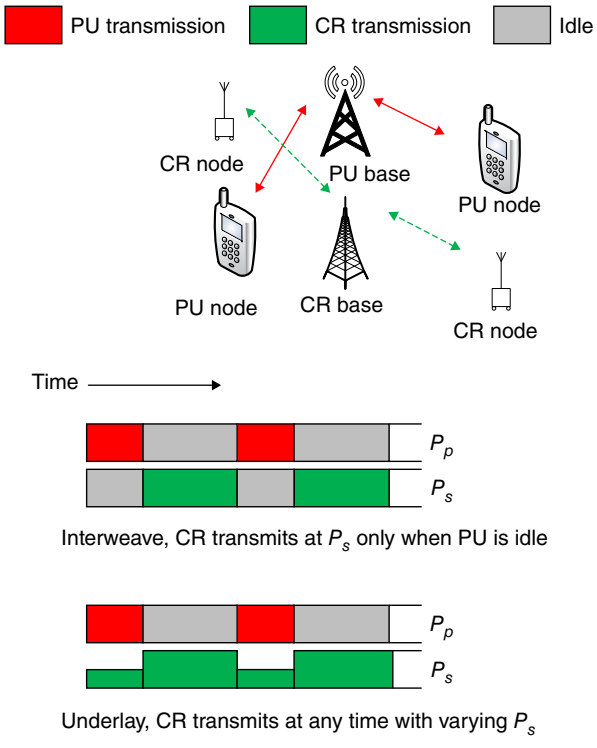

Figure 7.4 Comparison of interweave CR and underlay CR when the temporal opportunities are exploited.

Compared with the interweave system, the underlay system does not stop transmission when the PU is operating, as it is allowed to coexist with the PU, but it does need power adjustment. In other words, the transmission power of the interweave system can be considered as a discrete set of either zero or P_s, while the transmission power of the underlay system is within a continuous range depending on the interference limitation. The interweave system is suitable for high data rate or high-power applications, while the underlay system is suitable for low data rate or low-power applications.

In the overlay CR system, the CR user has full cooperation with the PU. For example, the PU transmitter can forward its signal to the CR and ask the CR to relay this signal to the PU receiver. The CR can combine its own signal with the relayed PU signal so that it can make use of this opportunity to deliver information to the CR receiver. In other words, the CR user helps the PU in exchange for the use of the licensed frequency band. In most cases, the CR needs to have important information about the PU network, such as its modulation scheme, its coding scheme, etc. Thus, in the overlay system, the CR and PU must trust each other. Figure 7.5 shows a diagram of an overlay CR system, where the CR cooperates with the PU for PU transmission in exchange for spectrum access. In this case, spectrum sensing is not needed, as the CR can get the spectrum occupancy information from the PU network directly.

Among these three systems, overlay has the full cooperation, underlay has the minimum cooperation, while interweave has no cooperation between the CR and the PU.

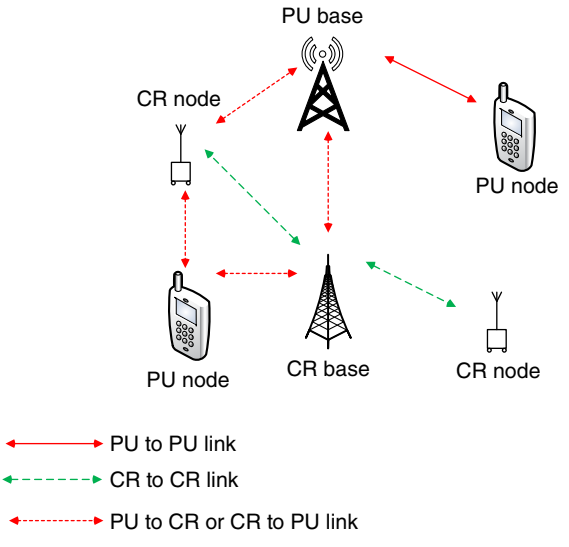

Figure 7.5 Diagram of an overlay CR system.

Consequently, interweave has the widest application. In an energy harvesting CR, if the overlay principle is used, spectrum sensing is not required. In this case, the energy harvesting CR designs will be much simpler, as there is only a tradeoff between energy harvesting and data transmission, which is very similar to the tradeoff between energy and rate discussed in Chapter 6. What makes CR unique is its spectrum sensing function. Thus, this chapter focuses on interweave and underlay CRs. Next, several commonly used spectrum sensing methods will be reviewed.

7.2.2 Spectrum Sensing Methods

7.2.2.1 Energy Detection

The most commonly used spectrum sensing method is energy detection (Urkowitz 1967). It stems from the detection theory in statistics.

In a static additive white Gaussian noise (AWGN) channel, the energy detection can be described by a binary hypothesis testing problem as

$$H_0(\text{channel free}) : \mathbf{y} = \mathbf{n} \tag{7.1a}$$

$$H_1(\text{channel occupied}) : \mathbf{y} = \mathbf{s} + \mathbf{n} \tag{7.1b}$$

where $\mathbf{y} = [y_1 \quad y_2 \cdots y_K]$ is the received sample, $\mathbf{n} = [n_1 \quad n_2 \cdots n_K]$ is the AWGN with mean zero and variance σ^2, and $\mathbf{s} = [s_1 \quad s_2 \cdots s_K]$ is the PU signal. This model can describe the case when a single CR performs spectrum sensing. In this case, K denotes the number of samples taken at different time instants at the CR. In this model, the elements in $\mathbf{s}$ are deterministic values.

There are many different detection rules. A commonly used rule is the maximum *a posteriori* rule. If the maximum *a posteriori* rule is used, the optimum detector can be designed as

$$P[H_0]f(\mathbf{y}|H_0) \underset{H_1}{\overset{H_0}{\gtrless}} P[H_1]f(\mathbf{y}|H_1) \tag{7.2}$$

where $P[H_0]$ and $P[H_1]$ are the *a priori* probabilities of H_0 and H_1, respectively, $f(\mathbf{y}|H_0) = \frac{1}{(2\pi\sigma^2)^{K/2}} e^{-\frac{\mathbf{y}\mathbf{y}^T}{2\sigma^2}}$ and $f(\mathbf{y}|H_1) = \frac{1}{(2\pi\sigma^2)^{K/2}} e^{-\frac{(\mathbf{y}-\mathbf{s})(\mathbf{y}-\mathbf{s})^T}{2\sigma^2}}$ are the likely functions, and $()^T$ represents the transpose operation. Thus, using the likelihood functions in the likelihood ratio test, one has

$$\mathbf{y}\mathbf{s}^T \underset{H_0}{\overset{H_1}{\gtrless}} \sigma^2 \ln \frac{P[H_0]}{P[H_1]} + \frac{1}{2}\mathbf{s}\mathbf{s}^T. \tag{7.3}$$

This is a coherent detector that requires knowledge of $\mathbf{s}$, which is not realistic in an interweave system. In fact, had $\mathbf{s}$ been known, there is no need for spectrum sensing, because the PU is there.

In a fading channel or in a static AWGN channel with random PU signals, which is normally the case in a wireless communications system, the values of $\mathbf{s}$ become random. Denote $\mathbf{s}$ as Gaussian random variables with mean zero and covariance matrix $\alpha^2\mathbf{I}$, where $\mathbf{I}$ is the $K \times K$ identity matrix, that is, the PU signal samples are independent and identically distributed with a common variance of α^2. Then, one has $f(\mathbf{y}|H_0) = \frac{1}{(2\pi\sigma^2)^{K/2}} e^{-\frac{\mathbf{y}\mathbf{y}^T}{2\sigma^2}}$ and $f(\mathbf{y}|H_1) = \frac{1}{[2\pi(\sigma^2+\alpha^2)]^{K/2}} e^{-\frac{\mathbf{y}\mathbf{y}^T}{2(\sigma^2+\alpha^2)}}$. Using them in (7.2) and calculating the likelihood ratio, one has the detector as

$$\mathbf{y}\mathbf{y}^T \underset{H_0}{\overset{H_1}{\gtrless}} D. \tag{7.4}$$

This is an energy detector, because $\mathbf{y}\mathbf{y}^T$ gives the energy of the received samples. If the maximum *a posteriori* rule is used, it can be shown that the detection threshold is given by $D = \frac{\sigma^2(2\sigma^2+2\alpha^2)}{\alpha^2} \ln\left[\frac{P[H_0]}{P[H_1]}\left(\frac{\sigma^2+\alpha^2}{\sigma^2}\right)^{K/2}\right]$.

One sees that, if the energy is larger than the threshold D, the decision is that the channel is occupied, while if the energy is smaller than the threshold D, the decision is that the channel is free. This agrees with intuition. One also sees that this detector needs knowledge of the average fading power and the noise power in the calculation of D. This leads to the noise uncertainty problem (Tandra and Sahai 2008), as the actual values of these parameters are not known in practice and they have to be estimated. The estimation error has a lower limit so that noise uncertainty will occur.

The model in (7.1) can also be adapted to describe the case when multiple CRs perform collaborative spectrum sensing. In this case, each CR takes one sample and K denotes the number of CRs. All these K samples are sent to the fusion center for a decision. If all the CR users take more than one sample in the time domain, the vectors will become matrices in (7.1) but the detection method will be similar.

The energy detector in (7.4) can be used to detect the spectrum holes in the time domain. For applications that exploit the spectrum opportunities in the spatial domain, one can use the distance-dependent path loss (Visotsky et al. 2005; Chen and Beaulieu

(2009). In this case, collaborative spectrum sensing has to be performed, where CR users at different locations sample the signal received from the licensed channel and then these samples are sent to a fusion center for a final decision. In this case, one has the binary hypothesis testing problem as

$$H_0(\text{channel free}) : \mathbf{z} \sim \mathcal{N}(\mu(R+\delta) \times \mathbf{1}, \sigma^2 \mathbf{\Sigma}) \tag{7.5a}$$

$$H_1(\text{channel occupied}) : \mathbf{z} \sim \mathcal{N}(\mu(R) \times \mathbf{1}, \sigma^2 \mathbf{\Sigma}) \tag{7.5b}$$

where $i = 1, 2, \cdots, N$ index samples taken at different CR users, $\mathcal{N}(\cdot, \cdot)$ represents a normal distribution, $\mathbf{z} = [z_1 \quad z_2 \cdots z_N]$ are the samples used for sensing, $\delta > 0$ and $\sigma^2 \mathbf{\Sigma}$ is the covariance matrix of $\mathbf{z}$, $\mathbf{z} = 10\log_{10}\mathbf{P}$ is the dB value of the average power received from the licensed channel by the N CR users, $\mathbf{P}$ is the actual value of the average power representing shadowing and is lognormally distributed with mean $\mu(r) \times \mathbf{1}$, $\mu(r)$ is the distance-dependent path loss, R is the safe distance so that the CR users only transmit data in the licensed frequency band of the PU when r is larger than R.

From (7.5), the detector can be derived as (Visotsky et al. 2005)

$$\frac{\mathbf{1}\times\mathbf{\Sigma}^{-1}\times\mathbf{z}^T}{\mathbf{1}\times\mathbf{\Sigma}^{-1}\times\mathbf{1}^T} \underset{H_0}{\overset{H_1}{\gtrless}} D \tag{7.6}$$

where D is the detection threshold. Using the maximum *a posteriori* detection rule, one has $D = \frac{\sigma^2}{(\mu(R)-\mu(R+\delta))\mathbf{1}\times\mathbf{\Sigma}^{-1}\times\mathbf{1}^T} \ln\frac{P[H_0]}{P[H_1]} + \frac{\mu(R)+\mu(R+\delta)}{2\mathbf{1}\times\mathbf{\Sigma}^{-1}\times\mathbf{1}^T}N$.

Using these detectors, two important performance measures can be defined: the probability of false alarm; and the probability of detection. The probability of false alarm is defined as

$$P_f = Pr\{H_1|H_0\}. \tag{7.7}$$

It represents the opportunity that the CR user has lost due to inaccurate sensing. Sometimes it is also called the probability of missed opportunity.

The probability of detection is defined as

$$P_d = Pr\{H_1|H_1\}. \tag{7.8}$$

It represents the protection the CR user can provide for the PU.

One sees that, in order to have a good sensing result, spectrum sensing should be designed in a way such that P_d is as large as possible to maximize the protection for the PU, while P_f is as small as possible to minimize the missed opportunity. Statistical theories have shown that the maximum *a posteriori* rule aims to minimize the overall error of $P[H_0]Pr\{H_1|H_0\} + P[H_1]Pr\{H_0|H_1\}$. However, within this overall error, it can be seen that, for CR systems, $Pr\{H_0|H_1\} = 1 - Pr\{H_1|H_1\}$ is more important than $Pr\{H_1|H_0\}$, as $Pr\{H_0|H_1\}$ determines the interference to the PU from the CR and for interweave systems the opportunistic spectrum access of the CR must be "non-interfering" according to the regulations. Thus, the maximum *a posteriori* rule cannot fulfill the regulatory requirements.

In most CR studies, the Neyman–Pearson detection rule is adopted, where one fixes the probability of false alarm $\Pr\{H_1|H_0\}$ as β, while minimizing $Pr\{H_0|H_1\}$ or maximizing P_d. Using the Neyman–Pearson rule, one needs to find the detection threshold in (7.4) and (7.6) by calculating P_f and fixing it at β.

In (7.4), under the hypothesis of H_0, $\mathbf{y}\mathbf{y}^T = \mathbf{n}\mathbf{n}^T$ follows a Gamma distribution with shape parameter $\frac{K}{2}$ and scale parameter $2\sigma^2$. Thus, one has the probability of false alarm as

$$\beta = 1 - G\left(D, \frac{K}{2}, 2\sigma^2\right) \tag{7.9}$$

where $G(D, \frac{K}{2}, 2\sigma^2) = \int_0^D \frac{1}{\Gamma(K/2)(2\sigma^2)^K} x^{K-1} e^{-x/(2\sigma^2)} dx$ is the cumulative distribution function of a Gamma distribution with shape parameter $K/2$ and scale parameter $2\sigma^2$. This gives the detection threshold as

$$D = G^{-1}\left(1 - \beta, \frac{K}{2}, 2\sigma^2\right) \tag{7.10}$$

where $G^{-1}(\cdot, \frac{K}{2}, 2\sigma^2)$ is the inverse function of $G(D, \frac{K}{2}, 2\sigma^2)$. Note that, the calculation of D in (7.10) does require knowledge of the noise power σ^2. Thus, it will suffer from noise uncertainty.

For (7.6), using a similar method, the detection threshold can be given by

$$D = \mu(R + \delta) + \frac{\sigma}{\sqrt{\mathbf{1}^T \times \mathbf{\Sigma}^{-1} \times \mathbf{1}}} Q^{-1}(\beta) \tag{7.11}$$

where $Q(x) = \frac{1}{\sqrt{2\pi}} \int_x^\infty e^{-t^2/2} dt$ is the Gaussian Q function, $Q^{-1}(\cdot)$ is the inverse of the Gaussian Q function, and β is the predetermined probability of false alarm. In this case, the calculation of the detection threshold D requires the noise power too. Thus, it still suffers from noise uncertainty.

In the Neyman–Pearson rule, the most important performance measure is the receiver operating characteristics (ROC), where P_f is the x axis and P_d is the y axis. Figure 7.6 gives an example of ROC for the energy detector in (7.4). One sees that a larger value K or a larger value of α^2/σ^2 improves the detection performance and that α^2/σ^2 has a larger impact on the performance.

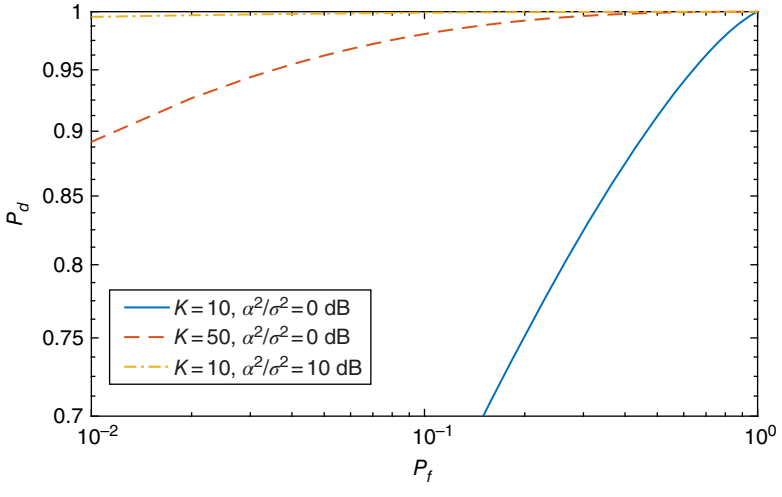

Figure 7.6 ROC of the energy detector in (7.4).

One sees from these expressions that the sensing accuracy depends on the number of samples K (or the number of users N in collaborative sensing) and the SNR $\frac{\alpha^2}{\sigma^2}$. Next, the feature-based detectors will be discussed.

7.2.2.2 Feature Detection

Energy is actually also a feature of the signal but feature detection uses other features of the signal, such as covariance and eigenvalues. In particular, the binary hypothesis testing problem is given by

$$H_0(\text{channel free}) : \mathbf{y} = \mathbf{n} \tag{7.12a}$$

$$H_1(\text{channel occupied}) : \mathbf{y} = \mathbf{s} + \mathbf{n} \tag{7.12b}$$

where $\mathbf{n}$ are independent and identically distributed Gaussian random variables with mean zero and variance σ^2, but the PU signals $\mathbf{s}$ are Gaussian random variables with mean zero and covariance matrix $\mathbf{\Sigma}$ and the (i,j)th element of $\mathbf{\Sigma}$ is $\rho^{|i-j|}$ with ρ being a constant $0 \leq \rho \leq 1$ and $|i-j|$ being the time difference between two samples. In this case, one has to assume correlated signals so that it can be distinguished from the uncorrelated noise samples. Otherwise, the feature detectors will fail. Most signals in practical systems are correlated, due to modulation, coding and other signal processing operations.

The sample covariance matrix of $\mathbf{y}$ is given by

$$R_y(K) = \begin{pmatrix} \vartheta(0) & \vartheta(1) & \cdots & \vartheta(L-1) \\ \vartheta(1) & \vartheta(0) & \cdots & \vartheta(L-2) \\ \vdots & \vdots & \vdots & \vdots \\ \vartheta(L-1) & \vartheta(L-2) & \cdots & \vartheta(0) \end{pmatrix}, \tag{7.13}$$

where $\vartheta(l) = \frac{1}{K}\sum_{k=1}^{K} y_k y_{k-l}$ is the sample covariance with a lag of l, and L is the smoothing factor. For pure noise or the null hypothesis, $R_y(K)$ will be very close to an identity matrix $\sigma^2\mathbf{I}$, while for the signal-plus-noise case or the alternative hypothesis H_1, $R_y(K)$ will be close to $\mathbf{\Sigma} + \sigma^2\mathbf{I}$. This allows us to detect the presence of the PU. Different properties of the sample covariance matrix can be used.

One can use the largest eigenvalue of $R_y(K)$. In this case, the sample covariance matrix is calculated from (7.13). The maximum eigenvalue of $R_y(K)$ is calculated from the sample covariance matrix. Then, it is compared with a detection threshold to be determined later. It can be derived that the probability of false alarm and the probability of detection are (Zeng et al. 2008)

$$P_f = 1 - TW_1\left(\frac{KD_{ME} - \gamma}{\epsilon}\right) \tag{7.14}$$

$$P_d = 1 - TW_1\left(\frac{KD_{ME} - \frac{K\rho_{max}}{\sigma^2} - \gamma}{\epsilon}\right) \tag{7.15}$$

where D_{ME} is the detection threshold of the maximum eigenvalue (ME) detector, $TW_1()$ represents the Tracy–Widom distribution of order 1 (Tracy and Widom 1996), $\epsilon = (\sqrt{K-1} + \sqrt{L})(\frac{1}{\sqrt{K-1}} + \frac{1}{\sqrt{L}})^{1/3}$, $\gamma = (\sqrt{K-1} + \sqrt{L})^2$, and ρ_{max} is the maximum eigenvalue of $R_y(K)$.

One can also use the ratio of the maximum eigenvalue to the minimum eigenvalue. In this case, first, the sample covariance matrix is calculated from (7.13). The maximum and minimum eigenvalues of $R_y(K)$ are calculated from the sample covariance matrix. Then, their ratio is calculated and compared with a detection threshold to be determined later. The probabilities of false alarm and detection can be derived as (Zeng and Liang 2009a)

$$P_f = 1 - TW_1\left[\frac{D_{MME}(\sqrt{K}-\sqrt{L})^2 - \gamma}{\epsilon}\right] \tag{7.16}$$

$$P_d = 1 - TW_1\left[\frac{KD_{MME} + \frac{K(D_{MME}\rho_{min} - \rho_{max})}{\sigma^2} - \gamma}{\epsilon}\right] \tag{7.17}$$

where D_{MME} is the detection threshold of the maximum-to-minimum eigenvalue (MME) detector, ρ_{min} is the minimum eigenvalues of $R_y(K)$, and other symbols are defined as before.

One can also use the ratio of the average energy to the minimum eigenvalue. In this case, the sample covariance matrix is calculated from (7.13). The minimum eigenvalue will be calculated from $R_y(K)$. Then, the average energy will be calculated as $\bar{E} = \frac{1}{K}\sum_{k=1}^{K}|y_k|^2$. After that, their ratio is calculated and compared with a detection threshold. The probabilities of false alarm and detection are derived as (Zeng and Liang 2009a)

$$P_f \approx Q\left[\frac{D_{EME}(\sqrt{K}-\sqrt{L})^2 - K}{\sqrt{2K}}\right] \tag{7.18}$$

$$P_d \approx Q\left\{\frac{D_{EME}[\rho_{min} + \frac{\sigma^2}{\sqrt{K}}(\sqrt{K}-\sqrt{L})] - \frac{tr[R_y(K)]}{L} - \sigma^2}{\sqrt{\frac{2}{K}}\sigma^2}\right\} \tag{7.19}$$

where D_{EME} is the detection threshold of the average energy to minimum eigenvalue (EME) detector and $tr[R_y(K)]$ is the trace of $R_y(K)$.

Finally, one can use the covariance of the sample directly. In this case, the sample covariance matrix is calculated from (7.13). Denote $R_y(i,j)$ as the element in the ith row and jth column. Then, the average covariance and the average variance are calculated as $T_1 = \frac{1}{K}\sum_{i=1}^{K}\sum_{j=1}^{K}|R_y(i,j)|$ and $T_2 = \frac{1}{K}\sum_{i=1}^{K}|R_y(i,i)|$, respectively. Finally, the ratio of T_1/T_2 is calculated and compared with a detection threshold. The probabilities are given by (Zeng and Liang 2009b)

$$P_f \approx 1 - Q\left\{\frac{\frac{1}{D_{COV}}[1 + (L-1)\sqrt{\frac{2}{K\pi}}] - 1}{\sqrt{2/K}}\right\} \tag{7.20}$$

$$P_d \approx 1 - Q\left[\frac{\frac{1}{D_{COV}} + \frac{r_L\sigma_s^2}{D_{COV}(\sigma_s^2+\sigma^2)} - 1}{\sqrt{2/K}}\right] \tag{7.21}$$

where D_{COV} is the detection threshold, $\sigma_s^2 = E[s^2(n)]$ is the average energy of the PU signal and $r_L = \frac{2}{L}\sum_{i=1}^{L-1}(L-i)|E[s(n)s(n-i)]/E[s^2(n)]|$. All these equations are obtained from random matrix theories.

Using the Neyman–Pearson rule, the detection thresholds can be determined by letting $P_f = \beta$ and solving the equations for D_{ME}, D_{MME}, D_{EME}, and D_{COV} in (7.14), (7.16), (7.18), and (7.20), respectively. For example, for the ME detector

$$D_{ME} = \frac{\epsilon}{K} \cdot TW_1^{-1}(1-\beta) + \frac{\gamma}{K} \tag{7.22}$$

from (7.14), where $TW_1^{-1}(\cdot)$ is the inverse function of the Tracy–Widom distribution of order 1.

One can see that (7.14), (7.16), (7.18), and (7.20) are only functions of the sample size K and the smoothing factor L. Consequently, the detection thresholds will be functions of K and L too. They will not depend on the noise power σ^2. Thus, they do not have the noise uncertainty problem.

On the other hand, in order to have an accurate estimate of the sample covariance, the sample size K often needs to be large. This incurs more computational complexity as well as longer sensing time. Thus, feature detectors are more complicated than the energy detector. Figure 7.7 compares different feature detectors in terms of their signal processing procedures.

Figure 7.8 compares the performances of different feature detectors, when $K = 100$ and $\sigma_s^2/\sigma^2 = 1$. The PU is assumed to leave or arrive during spectrum sensing with dynamic traffic (Chen et al. 2011b). The average arrival time and the average departure time are 4 s. One sees that the EME detector is the worst, while the ME detector is the best.

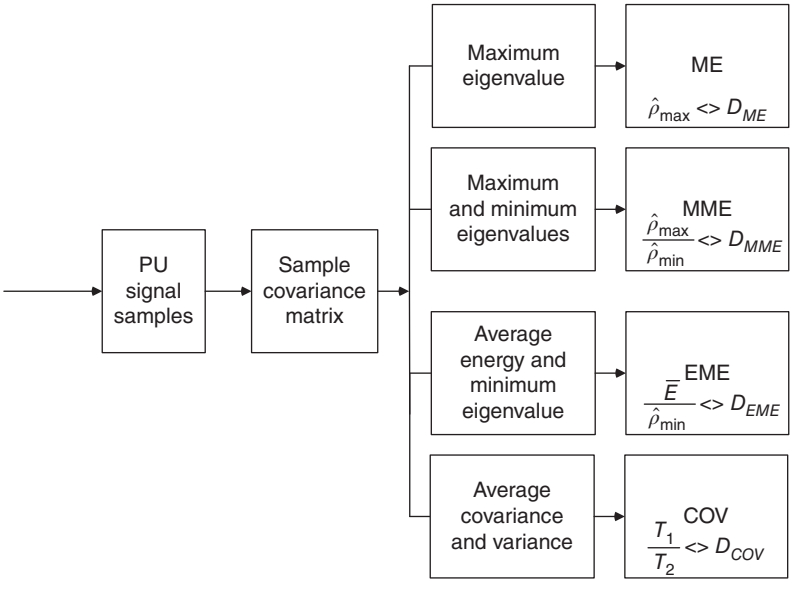

Figure 7.7 Comparison of different feature detectors.

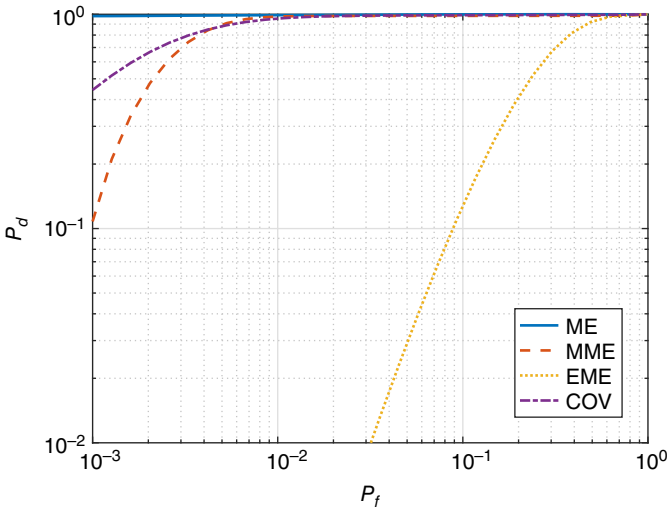

Figure 7.8 Performances of different feature detectors.

There are other feature detectors, such as cyclo-stationarity and spectral estimators. These are even more complicated. Also, feature detection can be combined with collaborative sensing to improve accuracies further. Most studies in energy harvesting CR adopt the energy detection due to its simplicity. In the following, without explicit explanation, spectrum sensing means energy detection.

7.3 Types of Energy Harvesting Cognitive Radio

With the background knowledge introduced in the previous section, from this section on, energy harvesting CR will be discussed. As mentioned before, the difference between energy harvesting CR and conventional CR is the extra energy harvesting capability at the CR. This not only adds a new function to the CR but also makes its energy supply random, leading to the energy causality problem.

7.3.1 Protocols

There are many different types of energy harvesting CR systems. They can be classified based on their protocols.

Some systems do not have an energy storage device at the CR so that the harvested energy must be used immediately. This is the "harvest-use" protocol (Kansal et al. 2007), similar to the variable-power transmission discussed in Chapter 4. In this protocol, the information rate is randomly changing, because the information rate is determined by the transmission power and the transmission power is determined by the random amount of energy harvested. Also, the instantaneous energy harvesting rate must always be larger than the energy consumption rate.

Other systems may have an energy storage device at the CR so that the harvested energy will be stored first before it can be used. The energy storage device serves as a

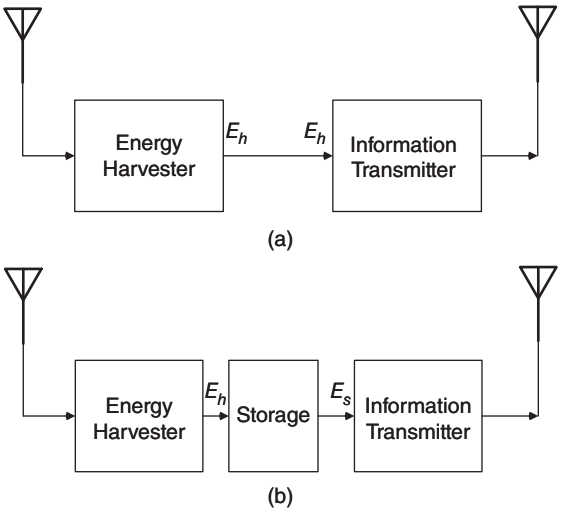

Figure 7.9 Comparison of (a) "harvest-use" and (b) "harvest-store-use".

buffer to level up the randomness in the amount of energy harvested. This is the "harvest-store-use" protocol (Yin et al. 2014), similar to the fixed-power transmission discussed in Chapter 4. In this case, it is possible to schedule energy harvesting and energy consumption, such as sensing and transmission, for the best resource allocation. Figure 7.9 compares these two protocols. The used energy E_s is not necessarily smaller than E_h because of previously stored energy. However, E_s is a fixed value, while E_h could be random.

The "harvest-use" protocol simplifies the energy harvesting CR design by removing energy storage, but this leads to variable rate. The "harvest-store-use" protocol requires energy storage, which increases the complexity of energy harvesting CR software and hardware, but it allows fixed-power and fixed-rate data performance with guaranteed QoS.

In the literature, the difference between these two protocols is reflected by different energy causality constraints. The optimization problems in the "harvest-use" protocol assume a battery with a size of 0 in the constraints. The optimization problems in the "harvest-store-use" protocol assume a battery with a finite size B in the constraints. As an extension of these studies, the optimization problems can also assume a battery with an infinite size in the constraints. These different constraints will lead to different optimal solutions. However, most studies in the literature have considered the "harvest-store-use" protocol with finite battery.

7.3.2 Energy Sources

The energy harvesting CR systems can also be classified based on the energy sources of the PU and the CR. Table 7.1 compares energy harvesting CR systems with different energy sources. Each reference in the table is only an example and the list is not exhaustive.

In some systems (Zhang et al. 2015), both PU and CR harvest energy from the same ambient source, for example, the Sun or the radio environment. In this case, the PU transmission is determined by the energy arrival process of the ambient source, which also determines the energy harvested by the CR. Essentially, sharing the same energy

Table 7.1 CR systems with different energy sources for PU and CR.

Reference	PU source	CR source
Zhang et al. (2015)	Ambient environment	Ambient environment
Azmat et al. (2018)	CR	PU
El Shafie et al. (2015)	Ambient environment	Fixed supply
Zhai et al. (2016a)	CR	Fixed supply
Zhang et al. (2016)	Fixed supply	Ambient environment
Lee and Zhang (2015)	Fixed supply	HAP
Zheng et al. (2014)	Fixed supply	PU
Usman and Koo (2014)	Fixed supply	PU and ambient

CR, cognitive radio; HAP, hybrid access point; PU, primary user.

source makes the PU and CR operations correlated and this correlation can be utilized to improve the sensing accuracy. However, this is only applicable to the case when the PU and CR use all the energy harvested, or the "harvest-use" protocol. In the cases when energy storage is used, this correlation will be less important or even negligible due to energy buffering.

In some systems (Azmat et al. 2018), PU and CR harvest energy from each other. When the PU transmits data, CR will harvest energy from this transmission. Similarly, when the CR transmits data over the spectrum holes, the PU harvests energy from the CR transmission too. In this case, since both PU and CR have three stages (data transmission, energy harvesting, and idle), more cases need to be considered for the sensing-throughput tradeoff at the CR and the PU to maximize the throughput and the harvested energy.

There are also systems where the CR does not harvest energy but the PU harvests energy from either the ambient source or the CR (El Shafie et al. 2015; Zhai et al. 2016a). They cannot be considered as energy harvesting CR systems, as the CR does not have the energy harvesting feature. Nevertheless, their designs will be related to energy harvesting CR designs, as the energy arrival affects the power supply of the PU. This in turn affects its data transmission due to the energy causality. The PU data transmission will then affect the spectrum sensing and the transmission opportunities at the CR.

In many studies on energy harvesting CR, such as Zhang et al. (2016), the PU has fixed energy supply, and only the CR harvests energy. In this case, as mentioned before, the energy arrival process determines the energy causality, while the PU traffic process determines the collision avoidance. Both need to be considered to optimize the resource allocation at the CR.

In Lee and Zhang (2015), the CR harvests energy from the secondary base station in the CR network. Thus, coordination between power transfer from the secondary base station and the data transmission from the CR users is required to make sure that there is enough energy for data transmission but also to make sure that the transmission power of the CR users will not cause noticeable interference to the PU.

In Zheng et al. (2014), the CR harvests energy from the PU. This is an incentive for the CR to forward its signal to the PR receiver. This idea is very similar to energy harvesting relaying to be discussed in the next chapter, except that the CR as a relay node is not in

the same network as the PU users as source and destination nodes. The benefit for the CR user is that the CR user can combine its own signal with the PU signal during the relaying to use the licensed frequency band. This is an overlay system. In both Zheng et al. (2014) and Lee and Zhang (2015) the power transfer is intentional to make the designs easier by only considering the collision avoidance, unlike the ambient source in Zhang et al. (2016).

In Usman and Koo (2014), the CR harvests energy from both the PU and the ambient source. This makes the system designs more complicated, because the PU traffic will not only affect the collision avoidance but also the energy causality. In any case, such a system may not be used in practice, as it needs two sets of energy harvesters with increased complexity.

In the literature, the majority of the studies focus on energy harvesting CR where the PU has fixed energy supply and the CR harvests energy from either an ambient source, or the PU, or the secondary base station. If the CR harvests energy from the ambient source, the energy arrival process is often considered in the joint optimization of transmission time and transmission power for resource allocation. If the CR harvests energy from the PU, the sensing time, the detection threshold and the spectrum access are often jointly optimized subject to energy and collision constraints. In the systems where the CR harvests energy from the secondary base station, the energy harvesting CR is much simpler, as only the collision constraint needs to be considered.

The rest of this chapter will discuss these energy harvesting CR systems. We will first discuss the energy harvesting CR systems that harvest energy from the secondary base station. Then, the CR systems that harvest energy from the PU signal and the CR systems that harvest energy from ambient sources will be discussed.

7.4 From the Secondary Base Station

Figure 7.10 shows a diagram of these energy harvesting CR systems. In this case, the CR system is actually a wireless powered communications system, similar to the hybrid access point (HAP) system discussed in Chapter 6. The only difference is that now this CR system has to share the licensed frequency band with the PU and hence, its downlink power transfer and uplink information delivery may be affected by the PU. Specifically, if the PU is transmitting at the same time as the CR downlink power transfer from the base station to the CR users, the CR users can harvest more energy but the PU receiver will be interfered by the CR wireless power. If the PU is transmitting at the same time as the CR uplink information delivery from the CR users to the base station, the base station will be interfered by the PU signal, while the PU receiver will be interfered by the CR users.

Consider an energy harvesting CR network with one base station and K CR nodes. The CR network operates at the same channel as the PU system with one PU transmitter and one PU receiver. Similar to the HAP system discussed in Chapter 6, the CR nodes do not have fixed power supply. In this case, the base station broadcasts wireless power in the downlink for τT seconds to charge the CR nodes, where T is the total link time. The harvested energy is then used by the CR nodes to transmit data to the base station in the uplink for $(1 - \tau)T$ seconds. There is a slight difference between this model and the model of the HAP system in Chapter 6, as the nodes

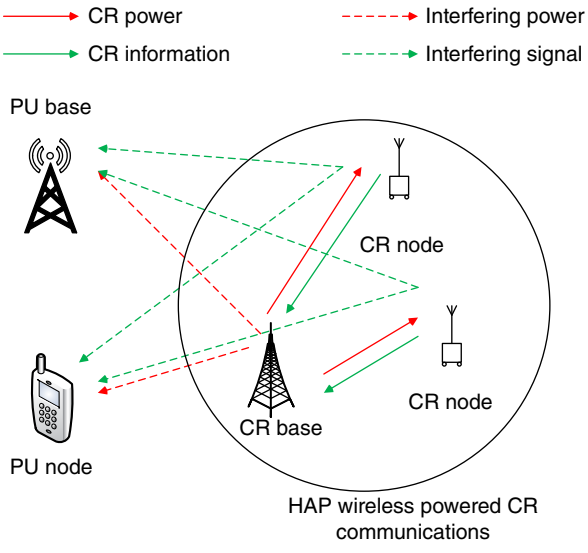

Figure 7.10 CR system that has its secondary base station as the energy source.

in the HAP system in Chapter 6 transmit their data sequentially with allocated time intervals of $\tau_1, \tau_2, \cdots, \tau_K$, while here all K nodes adopt simultaneous transmission during $(1-\tau)T$. Thus, the HAP system in Chapter 6 uses time-division-multiple-access (TDMA), while here the CR network can use code-division-multiple-access (CDMA) or orthogonal-frequency-division-multiple-access (OFDMA) that allow simultaneous transmission of multiple users. Non-orthogonal multiple access (NOMA) may also be used. The purpose of simultaneous transmission is to reduce the chance of interfering the PU as much as possible.

In the downlink, the received signals at the CR nodes can be expressed as

$$y_i = \sqrt{P_s} h_i s + \sqrt{P_p} g_i x + n_i \tag{7.23}$$

where $i = 1, 2, \cdots, K$ represents different CR nodes, P_s is the transmission power of the base station or the HAP, h_i is the channel gain from the base station to the ith CR node, s is the transmitted symbol of the base station, P_p is the transmission power of the PU transmitter, g_i is the channel gain from the PU transmitter to the ith CR node, x is the transmitted symbol of the PU, and n_i is the AWGN. In the following, assume that h_i and g_i are fixed complex values during each transmission but vary from transmission to transmission and that $E[|s|^2] = E[|x|^2] = 1$. Hence, the system operates in block fading channels with normalized symbols. Also, the noise is a complex Gaussian random variable with mean zero and variance $2\sigma^2$. An important assumption made in (7.23) is that the PU transmitter is always transmitting at a fixed transmission power. In some applications, the PU may have on–off traffic such that the PU term may not always be in (7.23). In this case, more complicated models for the PU term in (7.23), such as a Markov process, need to be used.

Using the signal in (7.23), the harvested energy at the ith CR node is given by

$$E_i = Q_i \tau = \eta_i (P_s |h_i|^2 + P_p |g_i|^2) \tau \tag{7.24}$$

where η_i is the conversion efficiency of the energy harvester at the ith CR node, Q_i is the harvested power, and $T = 1$ for convenience. One sees that the PU transmission leads

to more harvested energy at the CR node, compared with the HAP system discussed in Chapter 6.

The harvested energy in (7.24) is then used for the following data transmission in the uplink. Assume that e_i of the harvested energy is used, where $e_i = c_i E_i$ and $0 \le c_i \le 1$ indicates the part of harvested energy used for data transmission. The other part $(1 - c_i)$ E_i is saved for future transmissions. Thus, the transmission power of the ith CR is given by

$$P_i = \frac{e_i}{(1-\tau)} = \frac{\tau}{1-\tau} c_i \eta_i (P_s |h_i|^2 + P_p |g_i|^2). \tag{7.25}$$

The received signal at the base station in the uplink can be expressed as

$$y_0 = \sum_{i=1}^{K} \sqrt{P_i} u_i s_i + \sqrt{P_p} g_0 x + n_0 \tag{7.26}$$

where P_i is the transmission power of the ith CR node in (7.25), u_i is the channel gain from the ith CR node to the base station, s_i is the information transmitted by the ith CR node, g_0 is the channel gain from the PU transmitter to the base station, and n_0 is the AWGN with mean zero and variance $2\sigma^2$. Thus, the information rate in the uplink can be derived as

$$R = (1-\tau)\log_2 \left(1 + \frac{\sum_{i=1}^{K} P_i |u_i|^2}{2\sigma^2 + P_p |g_0|^2} \right). \tag{7.27}$$

In the derivation of (7.27), the multi-user interference has been ignored so that the total signal power is the sum of each user's power. One sees that the PU transmitter degrades the CR performance in the uplink due to interference.

The above derivations apply to any wireless powered system with interference. For CR systems, since the CRs operate with the PU using the underlay principle, the transmission powers of the base station and the CR nodes must be limited. Specifically, assume an interference temperature determined by a peak transmission power limit Γ at the PU, one has

$$P_s = \min \left(\frac{\Gamma}{|h_0|^2}, P_{max} \right) \tag{7.28}$$

where h_0 is the channel gain from the base station to the PU receiver such that the interference caused by the base station power transfer $P_s |h_0|^2$ is smaller than or equal to the limit Γ, and P_{max} is the maximum power that the base station can physically use.

Similarly, to limit interference caused by the CR nodes, one has

$$\sum_{i=1}^{K} P_i |v_i|^2 \le \Gamma \tag{7.29}$$

where v_i is the channel gain from the ith CR node to the PU receiver. Several points can be made. First, in (7.28) and (7.29), knowledge of h_0 and v_i is available at the base station and the ith CR node, respectively, in order to satisfy the interference temperature requirement. Secondly, (7.28) and (7.29) use a peak transmission power limit. One may also limit the average transmission power or the power outage probability. In this case, only the average fading power or the distribution are needed. Finally, there have been

Table 7.2 List of channel gains.

Symbols	Channels
g_0	From PU transmitter to CR base station
g_i	From PU transmitter to ith CR
h_0	From CR base station to PU receiver
h_i	From CR base station to ith CR
u_i	From ith CR to CR base station
v_i	From ith CR to PU receiver

CR, cognitive radio; PU, primary user.

a lot of channel gains defined in the above. Table 7.2 lists all the channel gains used in the discussion for clarity.

Putting all these equations together, the optimization problem in this energy harvesting CR system can be derived as

$$\max_{\tau,e_i}(1-\tau)\log_2\left(1+\frac{1}{1-\tau}\sum_{i=1}^{K}\frac{|u_i|^2e_i}{2\sigma^2+P_p|g_0|^2}\right) \tag{7.30}$$

$$0\le\tau\le 1 \tag{7.31}$$

$$0\le e_i\le E_i \tag{7.32}$$

$$\frac{1}{1-\tau}\sum_{i=1}^{K}|v_i|^2e_i<\Gamma. \tag{7.33}$$

A global optimization is difficult. Hence, a suboptimal solution to (7.30) can be derived in two steps. First, one fixes τ to $\hat{\tau}$ to have

$$\max_{e_i}(1-\hat{\tau})\log_2\left(1+\frac{1}{1-\hat{\tau}}\sum_{i=1}^{K}\frac{|u_i|^2e_i}{2\sigma^2+P_p|g_0|^2}\right) \tag{7.34}$$

$$0\le e_i\le\hat{\tau}Q_i \tag{7.35}$$

$$\frac{1}{1-\hat{\tau}}\sum_{i=1}^{K}|v_i|^2e_i<\Gamma. \tag{7.36}$$

This optimization problem can be solved using the method in Lee and Zhang (2015). Specifically, it was shown in Lee and Zhang (2015) that, for $0<\hat{\tau}<\frac{\Gamma}{\Gamma+\sum_{i=1}^{K}|v_i|^2Q_i}$, the optimum solution of e_i is given by

$$\hat{e}_i=\hat{\tau}Q_i \tag{7.37}$$

and for $\frac{\Gamma}{\Gamma+\sum_{i=1}^{k}|v_{(i)}|^2Q_{(i)}} < \hat{\tau} \le \frac{\Gamma}{\Gamma+\sum_{i=1}^{k-1}|v_{(i)}|^2Q_{(i)}}$, $k = 1, 2, \cdots, K$, the optimum solution of e_i is

$$\hat{e}_i = \begin{cases} \hat{\tau}Q_{(i)}, & i = 1, 2, \cdots, k-1 \\ \frac{1}{|v_{(i)}|^2}[(1-\hat{\tau})\Gamma - \hat{\tau}\sum_{i=1}^{k-1}|v_{(i)}|^2Q_{(i)}], & i = k \\ 0 & i = k+1, k+2, \cdots, K \end{cases} \tag{7.38}$$

where (i) indexes the ith largest value of $\frac{|u_i|^2}{(2\sigma^2+P_p|g_0|^2)|v_i|^2}$ by ordering all these K values according to $\frac{|u_{(1)}|^2}{(2\sigma^2+P_p|g_0|^2)|v_{(1)}|^2} > \cdots > \frac{|u_{(K)}|^2}{(2\sigma^2+P_p|g_0|^2)|v_{(K)}|^2}$. Thus, for any value of $\hat{\tau}$ between 0 and 1, it has been divided into $K+1$ intervals, from 0 to $\frac{\Gamma}{\Gamma+\sum_{i=1}^{K}|v_i|^2Q_i}$, from $\frac{\Gamma}{\Gamma+\sum_{i=1}^{K}|v_i|^2Q_i}$ to $\frac{\Gamma}{\Gamma+\sum_{i=1}^{K-1}|v_{(i)}|^2Q_{(i)}}$, until from $\frac{\Gamma}{\Gamma+\sum_{i=1}^{1}|v_{(i)}|^2Q_{(i)}}$ to 1. For each interval, the optimum value of $\hat{e}_i$ can be found.

The first step fixes τ to optimize e_i. Using the optimized e_i, in the second step, the optimum values of $\hat{e}_i$ are put back into (7.30) to replace e_i. The objective function is then only dependent on τ. Specifically, for $0 < \hat{\tau} < \frac{\Gamma}{\Gamma+\sum_{i=1}^{K}|v_i|^2Q_i}$, one has

$$R(\hat{\tau}) = (1-\hat{\tau})\log_2\left(1 + \frac{\hat{\tau}}{1-\hat{\tau}}\sum_{i=1}^{K}\frac{|u_i|^2Q_i}{2\sigma^2 + P_p|g_0|^2}\right) \tag{7.39}$$

and for $\frac{\Gamma}{\Gamma+\sum_{i=1}^{k}|v_{(i)}|^2Q_{(i)}} < \hat{\tau} \le \frac{\Gamma}{\Gamma+\sum_{i=1}^{k-1}|v_{(i)}|^2Q_{(i)}}$, $k = 1, 2, \cdots, K$, one has

$$R(\hat{\tau}) = (1-\hat{\tau})\log_2\left\{1 + \frac{\hat{\tau}}{1-\hat{\tau}}\sum_{i=1}^{k}\frac{|u_{(i)}|^2Q_{(i)}}{2\sigma^2 + P_p|g_0|^2} + \frac{1}{1-\hat{\tau}}\frac{|u_{(k)}|^2}{(2\sigma^2+P_p|g_0|^2)|v_{(k)}|^2}[(1-\hat{\tau})\Gamma - \hat{\tau}\sum_{i=1}^{k-1}|v_{(i)}|^2Q_{(i)}]\right\}. \tag{7.40}$$

Finally, (7.39) and (7.40) can be used to find the optimum value of $\hat{\tau}$, which can then be used in (7.37) and (7.38) to find the optimum value of $\hat{e}_i$ in the second iteration. The iterative process continues until the updated objective function is within a threshold of the previous objective function.

There is no analytical solution due to the non-linearity of the functions in the expression but numerical methods can be used to search for the optimum values. Figure 7.11 gives an example of $R(\hat{\tau})$ for illustration purposes, where $K = 5, \eta_i = 1, P_s = 1, P_p = 0.01$, $h_i = g_i = u_i = v_i = g_0 = 1, \Gamma = 1$, and $2\sigma^2 = 1$. An optimum value of $\hat{\tau}$ can be seen from the figure. More details for the above results can be found in Lee and Zhang (2015).

Other optimizations can also be performed in (7.30) under different conditions. For example, if all the harvested energy is used for data transmission, $c_i = 1$. Then, one can optimize τ only. This optimization is very similar to the HAP system in Chapter 6, except that there is an additional constraint on the transmission power. One may also optimize P_s and τ jointly, or P_s, P_p and τ jointly. These will lead to a joint time and power allocation problem. Also, instead of fixing the downlink time τ and the uplink time $1-\tau$, the two operation modes of the CR network can be adapted to the fading state so that uplink information delivery and downlink power transfer only operate when necessary (Ji et al. 2017).

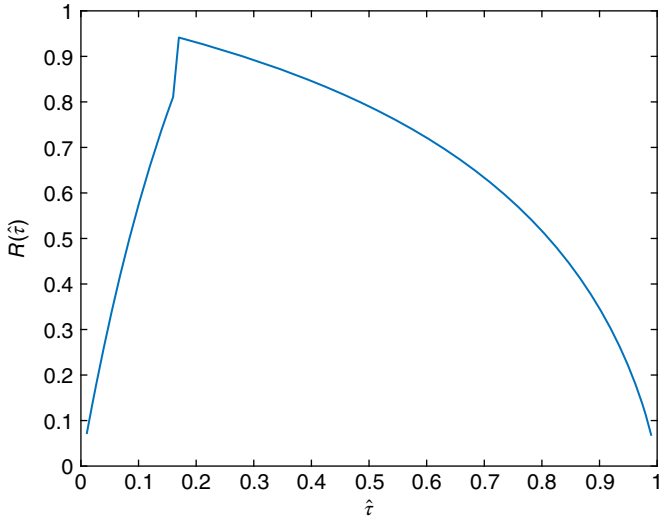

Figure 7.11 $R(\hat{\tau})$ versus $\hat{\tau}$.

The results for TDMA can be obtained in a similar way. In this case, each CR node transmits within the allocated time sequentially. This will make the optimization problem more complicated, as instead of τ one will have τ_1, τ_2, and τ_K for the K CR nodes, where $\tau_1 + \tau_2 + \cdots + \tau_K = 1 - \tau$. The optimal value still exists but the solution is difficult to obtain. For example, in Xu and Li (2017), K CR nodes were assumed to transmit during τ_1, τ_2 until τ_K, similar to the HAP wireless powered system discussed in Chapter 6. In this case, the ith CR node has a rate of

$$R_i = \tau_i \log_2 \left[1 + \frac{\eta_i (P_s |h_i|^2 + P_p |g_i|^2) |u_i|^2 \tau}{\tau_i (2\sigma^2 + P_p |g_0|^2)} \right] \tag{7.41}$$

and the total interference to the PU is

$$Q = \frac{1}{T} \left(P_s |h_0|^2 \tau + \sum_{i=1}^{K} P_i |v_i|^2 \tau_i \right). \tag{7.42}$$

The optimization problem becomes (Xu and Li 2017)

$$\max_{\tau, \tau_1, \cdots, \tau_K, P_s} \left\{ \sum_{i=1}^{K} R_i \right\} \tag{7.43}$$

$$Q \leq Q_{max} \tag{7.44}$$

$$P_s \leq P_{max}, P_s \tau \leq P_{avg} \tag{7.45}$$

$$\tau + \sum_{i=1}^{K} \tau_i = 1 \tag{7.46}$$

where Q_{max} is the peak interference power allowed by the PU, P_{max} is the maximum transmission power for CR, and P_{avg} is the average transmission power for CR.

This is a complicated problem. In Cheng et al. (2017) the proportional fairness was also considered, where the sum rate becomes $\sum_{i=1}^{K} \omega_i \log(R_i)$ for optimization, where ω_i is the weighting factor for the ith CR node.

In the above discussion, the underlay principle is considered. One can easily extend the results to the interweave principle or the overlay principle. In fact, Lee and Zhang (2015) have also studied the overlay principle, where the CR system has more knowledge about the PU transmitter and the PU receiver. It was reported by Lee and Zhang (2015) that the overlay principle outperforms the underlay principle, as expected, as extra knowledge is available and extra coordination between CR and PU can be performed, but this also leads to higher complexity. For the interweave principle, spectrum sensing will be required, in addition to uplink data transmission and downlink power transfer. Thus, more cases need to be discussed.

In summary, the above discussion gives an example of how the energy harvesting CR system works by harvesting energy from the base station. The key is the interference temperature imposed by the PU that limits the transmission power of both the CR node and the base station, giving different optimum solutions compared with the wireless powered systems without spectrum sharing in Chapter 6. Next, the energy harvesting CR systems that harvest energy from the PU will be discussed.

7.5 From the Primary User

7.5.1 Conventional PU

Figure 7.12 shows the diagram of an energy harvesting CR system where the CR harvests energy from the signal transmitted by a conventional PU system without wireless power. In this case, the energy harvesting CR has three operation modes: transmission mode; harvesting mode; and idle mode. The PU transmitter is powered by either batteries or

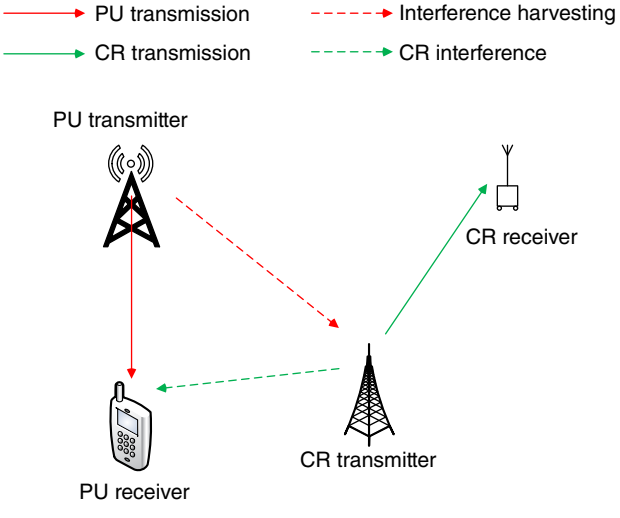

Figure 7.12 CR system that harvests energy from the PU.

mains connections and is randomly distributed in the space. The area around the PU transmitter is divided into three rings. The inner most ring is called the harvesting zone, where the PU signal is the strongest so that it is good for the CR to harvest the energy. The outer most ring is called the guard zone, where the PU signal is the weakest so that it is good for the CR to transmit the data by exploiting the spatial opportunities. The ring between the harvesting zone and the guard zone is neither good for harvesting nor good for transmission. The CR is also randomly distributed. If the CR finds itself in the harvesting zone and its battery is not full, it will switch to the harvesting mode to harvest energy from the PU signal. If the CR finds itself in the guard zone and it has sufficient energy, it will switch to the transmission mode to transmit data on the licensed channel. In other cases, the CR will switch to the idle mode. We are interested in finding out the transmission probability of the CR (Lee et al. 2013).

Also, this discussion assumes that the distance between the CR and the PU is known through some localization and feedback channel so that the CR switches its mode based on the distance. In this case, spectrum sensing is not needed. If the location information is not available, spectrum sensing will be required, as discussed in Section 7.2.

One can see from the above description that this is actually an underlay spectrum sharing system, where the CR utilizes the spectrum holes in the spatial domain (the guard zone) for opportunistic spectrum access. Also, this is a "harvest-store-use" protocol, as the CR only transmits when it has the required energy. Compared with a conventional CR system, the random location of the CR node makes its harvesting time random and the random signal from the PU also makes the amount of harvested energy random so that the energy supply at the CR is dynamic.

Consider a CR network, where the active PU transmitters (PUs that are transmitting data) follow a homogeneous Poisson point process with density λ_p and the CR transmitters follow another independent homogeneous Poisson point process with density λ_c. The PU transmitters transmit signals at a fixed power of P_p and the CR transmitters transmit signals at a fixed power of P_s. The distance between PU transmitter and receiver is d_p, and the distance between CR transmitter and receiver is d_c. Each PU transmitter has an associated guard zone, which is centered around itself with a radius of r_g. The probability that a CR transmitter is in a guard zone of any PU transmitter, or that there is no PU transmitter in the zone centered around the CR transmitter with radius r_g is given by (Lee et al. 2013)

$$p_g = e^{-\pi r_g^2 \lambda_p} \tag{7.47}$$

as the number of PU transmitters follows a Poisson distribution with mean $\pi r_g^2 \lambda_p$, where πr_g^2 is the area of the circle, and λ_p is the density of the PU transmitters.

Most energy harvesters have an activation level or sensitivity, below which the energy from the PU is too small to be harvested. As the signal strength decreases with the distance, if the CR wants to harvest energy from the PU signal, this sensitivity can be translated into a harvesting zone centered around the PU transmitter. Denote r_h as the distance from the PU transmitter beyond which no energy can be harvested. Thus, the disc around the PU transmitter with a radius of r_h is the harvesting zone, and the smallest power at the edge of this zone is $P_p r_h^{-\alpha}$, where P_p is the PU transmission power defined before, α is the path loss exponent, and $r_h^{-\alpha}$ is the path loss at a distance of r_h. The probability that a CR transmitter is in a harvesting zone of any PU transmitter, or that there is at least one PU transmitter in the zone centered around the CR transmitter with radius

r_h is given by (Lee et al. 2013)

$$p_h = 1 - e^{-\pi r_h^2 \lambda_p} \tag{7.48}$$

as the number of PU transmitters inside this disc follows a Poisson distribution with mean $\pi r_h^2 \lambda_p$, where πr_h^2 is the area of the disc. The minimum harvested power is then $\eta P_p r_h^{-\alpha}$ at the edge of the zone, where η is the conversion efficiency of the energy harvester.

In the above, several assumptions have been made. First, $\lambda_p \ll \lambda_s$ and hence there are far less PU transmitters than CR transmitters. Also, $d_p \ll r_g$, which means that the PU receiver is very close to the PU transmitter such that r_g is enough to protect both of them. Finally, $r_h \ll r_g$ so that the harvesting zone πr_h^2 is much smaller than the guard zone πr_g^2.

The CR transmitter only transmits data when it is in the guard zone and it has the required energy in the battery. Thus, the probability of transmission is given by

$$p_t = p_b p_g \tag{7.49}$$

where p_b is the probability that the battery is full. The probability p_b is discussed in the following. The minimum harvested power is $\eta P_p r_h^{-\alpha}$, and the required power for transmission at the CR is P_s. Thus, the CR transmitter needs at least $M = \lceil \frac{P_s}{\eta P_p r_h^{-\alpha}} \rceil$ times of charging to be ready for transmission. This means that the CR transmitter may need to be in the harvesting zone at most M times during M time slots, if it is too far away from the PU transmitter.

When $0 < P_s \leq \eta P_p r_h^{-\alpha}$, $M = 1$. Thus, the battery state is either 0 or P_s with at most one charge. The charging process can be modeled as a two-state Markov chain with state transition probability matrix

$$\begin{bmatrix} 1 - p_h & p_h \\ p_g & 1 - p_g \end{bmatrix} \tag{7.50}$$

where the probability from 0 to 0 is $1 - p_h$, the probability from 0 to P_s is p_h when the CR transmitter is in the harvesting zone, the probability from P_s to 0 is p_g when the CR transmitter is outside the guard zone and performs one data transmission, and the probability from P_s to P_s is $1 - p_g$ where the CR has full battery but is inside the guard zone. This model has been discussed in Chapter 3 as well. The average probability of full battery p_b is given by the steady-state probability of P_s and can be calculated as (Lee et al. 2013)

$$p_b = \frac{p_h}{p_h + p_g}. \tag{7.51}$$

When $\eta P_p r_h^{-\alpha} < P_s \leq 2\eta P_p r_h^{-\alpha}$, $M = 2$. In this case, the CR transmitter needs at most two charges to be ready for data transmission. If it is close to the PU transmitter, enough power can be harvested in one charge. If it is too far away from the PU transmitter, two charges are required. Thus, the battery state is either 0, or between $\frac{1}{2}P_s$ and P_s, or P_s. It has three states and thus, can be described by a three-state Markov chain with state transition probability matrix

$$\begin{bmatrix} 1 - p_h & p_2 & p_1 \\ 0 & 1 - p_h & p_h \\ p_g & 0 & 1 - p_g \end{bmatrix} \tag{7.52}$$

where $p_2 = p_h - p_1 = e^{-\pi h_1^2 \lambda_p} - e^{-\pi r_h^2 \lambda_p}$ is the probability from 0 to a value between $\frac{P_s}{2}$ and P_s when the CR transmitter is the harvesting zone but not close enough to the PU transmitter, $p_1 = 1 - e^{-\pi h_1^2 \lambda_p}$ is the probability from 0 to P_s when the CR transmitter is close enough to the PU transmitter such that only one charge is needed, $h_1 = (\frac{P_s}{\eta P_p})^{-\frac{1}{\alpha}}$ is the distance to the PU transmitter that determines if one charge is enough, and other probabilities are defined as before. The average probability of full battery p_b can again be obtained from the steady-state probability of P_s and is given by (Lee et al. 2013)

$$p_b = \frac{p_h}{p_h + p_g(1 + \frac{p_2}{p_h})}. \tag{7.53}$$

When $2\eta P_p r_h^{-\alpha} < P_s, M > 2$. This case is quite complicated. The probability of full battery can only be bounded as (Lee et al. 2013)

$$\frac{p_1 + p_2'}{(p_1 + p_2') + p_g(1 + \frac{p_2'}{p_1 + p_2'})} < p_b < \frac{p_h}{p_h + p_g(1 + \frac{p_3 + p_2'}{p_h})} \tag{7.54}$$

where $p_2' = e^{-\pi h_1^2 \lambda_p} - e^{-\pi h_2^2 \lambda_p}$, $p_3 = p_h - p_1 - p_2' = e^{-\pi h_2^2 \lambda_p} - e^{-\pi r_h^2 \lambda_p}$, and $h_2 = (\frac{P_s}{2\eta P_p})^{-\frac{1}{\alpha}}$ is the distance to the PU transmitter that determines if one charge to the CR transmitter is enough.

Next, the outage probability of the PU receiver and the CR receiver will be discussed. This will determine the information rate later. For the PU receiver, the outage probability can be defined as

$$P_{OP} = Pr\left\{ \frac{|h|^2 P_p |d_p|^{-\alpha}}{I_p + I_c + 2\sigma^2} < \Gamma_p \right\} \tag{7.55}$$

where h is the channel gain between the PU transmitter and the PU receiver and is a complex Gaussian random variable with mean 0 and variance 0.5 so that $|h|^2$ is an exponential random variable with mean 1, I_p is the interference power caused by other active PU transmitters in the area, I_c is the interference power caused by other active CR transmitters nearby, $2\sigma^2$ is the noise power, and Γ_p is the interference temperature in terms of signal-to-interference-plus-noise ratio (SINR) that the PU can tolerate. It has been derived in Lee et al. (2013) that

$$P_{OP} = 1 - e^{-a_p} \tag{7.56}$$

where $a_p = [\lambda_p + p_t \lambda_c (P_s/P_p)^{2/\alpha}] \Gamma_p^{2/\alpha} d_p^2 m + \frac{\Gamma_p d_p^\alpha 2\sigma^2}{P_p}$, $m = \pi \frac{2}{\alpha} \Gamma(\frac{2}{\alpha}) \Gamma(1 - \frac{2}{\alpha})$ and $\Gamma(\cdot)$ is the Gamma function.

Similarly, the outage probability at the CR receiver can be defined as

$$P_{OC} = Pr\left\{ \frac{|g|^2 P_s d_c^{-\alpha}}{I_p + I_c + 2\sigma^2} < \Gamma_c \right\} \tag{7.57}$$

where g is the fading gain between the CR transmitter and the CR receiver, and $|g|^2$ is an exponential random variable with mean 1. This outage probability was also derived in Lee et al. (2013) as

$$P_{OC} \approx 1 - \frac{1}{p_g} e^{-a_c} \tag{7.58}$$

where $a_c = [\lambda_p(P_s/P_p)^{-2/\alpha} + p_t\lambda_c]\Gamma_c^{2/\alpha} d_c^2 m + \frac{\Gamma_c d_c^\alpha 2\sigma^2}{P_s}$. Details of the derivations of (7.56) and (7.58) can be found in Lee et al. (2013) and its relevant references.

Finally, the optimization problem is described as

$$\max_{P_s,\lambda_c}\{p_t\lambda_c \log_2(1+\Gamma_c)\} \tag{7.59}$$

$$P_{OP} \le \epsilon_p \tag{7.60}$$

$$P_{OC} \le \epsilon_c. \tag{7.61}$$

One sees that this problem aims to maximize the information rate with respect to the CR transmission power and CR density, subject to a constraint on the PU performance, which can be considered as the power outage constraint in underlay systems, and a constraint on the CR outage performance. In some applications, the CR does not have any QoS requirements and the system works in the best-effort manner. In this case, the constraint on the CR outage can be removed.

For interference-limited scenarios where the noise power $2\sigma^2$ can be ignored and $M \le 2$, the optimal solution to (7.59) can be derived analytically as (Lee et al. 2013)

$$R_{max} = \frac{b_c(b_p - m\Gamma_p^{2/\alpha} d_p^2 \lambda_p)}{\Gamma_c^{2/\alpha} d_c^2 b_p m} \log_2(1+\Gamma_c) \tag{7.62}$$

where $b_c = -\ln[(1-\epsilon_c)p_g]$ and $b_p = -\ln(1-\epsilon_p)$. The optimal power and density are

$$P_s^{opt} = \frac{\Gamma_c}{\Gamma_p}\left(\frac{d_c}{d_p}\right)^\alpha \left(\frac{b_c}{b_p}\right)^{-\alpha/2} P_p \tag{7.63}$$

and

$$\lambda_c^{opt} = \frac{b_c(b_p - m\Gamma_p^{2/\alpha} d_p^2 \lambda_p)}{p_t P_s^{opt} \Gamma_c^{2/\alpha} d_c^2 b_p m}, \tag{7.64}$$

respectively. Figure 7.13 show the maximum information rate in (7.62) with respect to λ_p. In this case, $d_p = d_c = 2$, $\alpha = 3$, $\Gamma_p = \Gamma_c = 7$, and $r_g = 2$. One sees that it increases with ϵ_p or ϵ_c but ϵ_c has a larger impact. This means that one can trade the CR outage performance for the CR rate performance. However, in general, the rate is very low. More details on the above results can be found in Lee et al. (2013).

In the case when the CR does not have any QoS requirement such that the constraint on the CR outage is dropped, one also has

$$\max_{P_s,\lambda_c}\{p_t\lambda_c \log_2(1+\Gamma_c)\} \tag{7.65}$$

$$P_{OP} \le \epsilon_p. \tag{7.66}$$

The maximum rate can be derived as

$$R_{max} = \log_2(1+\Gamma_c)\left(\frac{P_p}{P_s^{opt}}\right)^{2/\alpha}\left(\frac{b_p - \Gamma_p d_p^\alpha 2\sigma^2/P_p}{\Gamma_p^{2/\alpha} d_p^2 m} - \lambda_p\right) \tag{7.67}$$

and the optimum density is given by

$$\lambda_c^{opt} = \frac{1}{p_t(P_s^{opt})}\left(\frac{P_p}{P_s^{opt}}\right)^{2/\alpha}\left(\frac{b_p - \Gamma_p d_p^\alpha 2\sigma^2/P_p}{\Gamma_p^{2/\alpha} d_p^2 m} - \lambda_p\right) \tag{7.68}$$

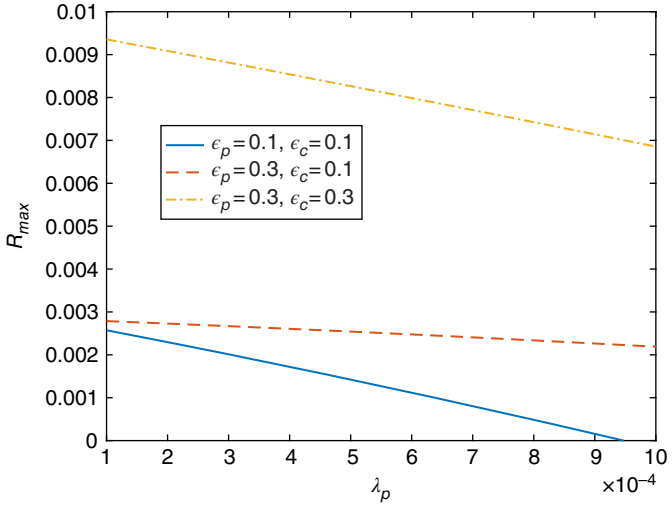

Figure 7.13 The optimum information rate in (7.62) versus λ_p.

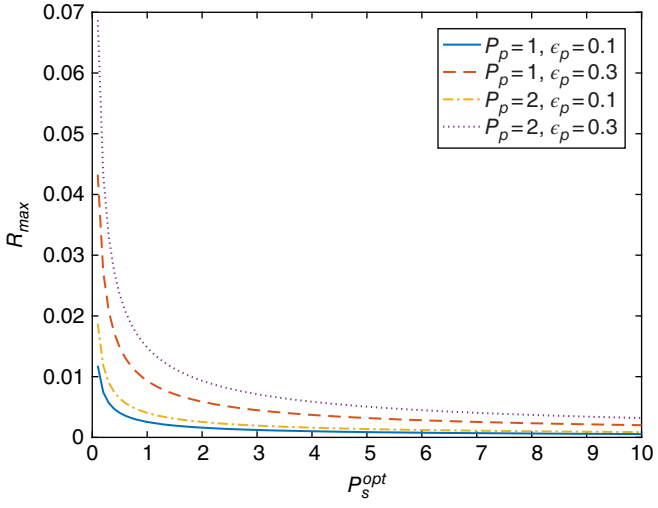

Figure 7.14 The optimum information rate in (7.67) versus P_s^{opt}.

where $p_t(P_s^{opt})$ is calculated by replacing P_s with P_s^{opt} in the expression of p_t. The optimum transmission power P_c^{opt} should be as small as possible, as expected, as there is no constraint on the CR outage (no minimum requirement on the CR performance) so that from the PU's point of view (the PU outage constraint), it should be as small as possible. Figure 7.14 shows the relationship between R_{max} and P_s^{opt} in (7.67). One sees that the transmission power of the CR can be traded for its rate. However, this tradeoff is only useful when the transmission power is small. For large transmission power, the decrease of the transmission power does not lead to noticeable increase of the rate.

Similarly, one could remove the constraint on the PU outage and conduct the optimization with the CR outage only. In this case, it can be shown that the optimum transmission power of the CR transmitter should be as large as possible, as expected. Details can be found in Lee et al. (2013).

Using (7.59), other optimization problems can also be formulated. For example, one may optimize the radius of the harvesting zone r_h and the radius of the guard zone r_g for fixed transmission power of P_s and fixed density of λ_c. This will be useful for CR applications with a fixed number of nodes and fixed transmission power due to hardware limitations.

The above design takes advantage of the spectrum holes in the spatial domain. One can also extend these results to the spectrum holes in the time domain. In this case, the PU and the CR are mixed in the space and the PU traffic is dynamic in time. Thus, the received power from the PU transmitter will be sampled at different time instants to decide when the licensed channel will be free and when the licensed channel will be occupied using spectrum sensing. If the channel is free and the battery of the CR is sufficient, the CR node will switch to the transmission mode. If the channel is occupied and the battery of the CR is not full, it switches to the harvesting mode. In other cases, it stays idle. This is very similar to the system discussed above where the channel status is determined by the distance instead. Such studies can be found in Pratibha et al. (2017).

One can also extend the above results to the interweave principle. In this case, the first energy detection method in Section 7.2.2.1 can be used to find the spectrum holes in the time domain, while the second energy detection method in Section 7.2.2.2 can be used to find the spectrum holes in the space domain. Then, the throughput and the harvested energy will be determined by the probabilities of false alarm and detection. The overlay principle can also be used. The result is very similar to energy harvesting relaying. Also, the above use the "harvest-store-use" protocol. The CR uses a fixed transmission power. One can also adopt the "harvest-use" protocol, where the CR uses a variable transmission power. In this case, $p_t = p_g$ will simplify the designs.

7.5.2 Wireless Powered PU

The previous subsection has considered the case when the PU is powered in a conventional way, such as batteries and mains connections. In this subsection, the PU also uses wireless power and thus is a HAP system as discussed in Chapter 6. Figure 7.15 shows a diagram of the system considered, where the PU network assumes a HAP structure using wireless power.

From Figure 7.15, we consider a wireless powered PU network with one access point (AP) and N PUs. These N PUs harvest energy from the AP for a time duration of τ_0. The harvested energy is used to transmit data from the PUs to the AP during τ_n, where τ_n represents the time duration allocated to the nth PU, $n = 1, 2, \cdots, N$, and $\tau_0 + \sum_{n=1}^{N} \tau_n = T$ is the total time. Meanwhile, CRs operate in the same area on the same channel. We consider one CR transmitter and one CR receiver. When the AP transfers energy to the PUs during τ_0, the cognitive transmitter transmits its own data to the cognitive receiver. When the PUs send data to the AP during $\tau_1, \tau_2, ..., \tau_N$, the cognitive transmitter starts to harvest energy from these transmissions. Finally, when the PU network is idle so that neither the AP is transferring energy nor the PUs are transmitting data, the cognitive

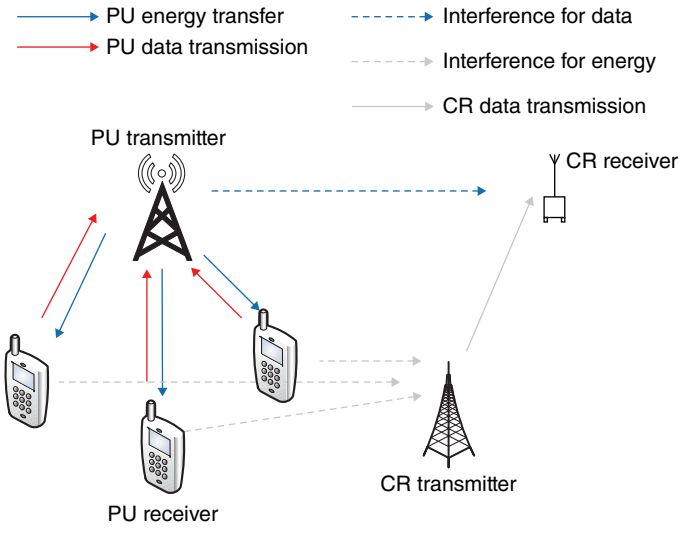

Figure 7.15 Diagram of energy harvesting CR where the PU uses wireless power.

transmitter uses this opportunity to transmit its data to the cognitive receiver. Denote this time as τ_{free}. Thus, the CR needs to detect the status of the PU network to decide its strategy. This detection could be erroneous so that several scenarios need to be discussed.

Assume that the transmission power of the AP for energy transfer to the PUs is much higher than the transmission power of the PUs for data transmission to the AP. This is normally the case, because the energy receiver has a much lower sensitivity than the information receiver. To this end, we define two decision thresholds as λ_1 and λ_2, where $\lambda_2 > \lambda_1$. Using energy detection, from Section 7.2.2, the detection variable is $T = \sum_{k=1}^{K} |y_k|^2$, where y_k is the received signal from the PUs or the AP at the CR. The PU network has three statuses based on energy detection:

$$
\begin{aligned}
&H_0 : \text{Neither AP nor PUs are transmitting } \Rightarrow\ T < \lambda_1 \\
&H_1 : \text{PUs are transmitting data } \Rightarrow\ \lambda_1 < T < \lambda_2 \\
&H_2 : \text{AP is transferring energy } \Rightarrow\ T > \lambda_2
\end{aligned}
$$

The probabilities of detection and false alarm for each status can be derived as in the following. For H_0,

$$
\begin{aligned}
P(H_2|H_0) &= P(T > \lambda_2|H_0) = \frac{\Gamma(K, \frac{\lambda_2}{2\sigma^2})}{\Gamma(K)} \\
P(H_1|H_0) &= P(\lambda_1 < T < \lambda_2|H_0) = \frac{\Gamma(K, \frac{\lambda_1}{2\sigma^2})}{\Gamma(K)} - \frac{\Gamma(K, \frac{\lambda_2}{2\sigma^2})}{\Gamma(K)} \\
P(H_0|H_0) &= 1 - P(H_1|H_0) - P(H_2|H_0)
\end{aligned}
$$

where $2\sigma^2$ is the noise power, $\Gamma(\cdot, \cdot)$ is the upper incomplete Gamma function, and $\Gamma(\cdot)$ is the Gamma function.

Similarly, for H_1, one has

$$P(H_2|H_1) = P(T > \lambda_2|H_1) = Q_K(\sqrt{2\gamma_1}, \sqrt{\lambda_2})$$
$$P(H_1|H_1) = P(\lambda_1 < T < \lambda_2|H_1) = Q_K(\sqrt{2\gamma_1}, \sqrt{\lambda_1}) - Q_K(\sqrt{2\gamma_1}, \sqrt{\lambda_2})$$
$$P(H_0|H_1) = 1 - P(H_1|H_1) - P(H_2|H_1)$$

and for H_2,

$$P(H_2|H_2) = P(T > \lambda_2|H_2) = Q_K(\sqrt{2\gamma_2}, \sqrt{\lambda_2})$$
$$P(H_1|H_2) = P(\lambda_1 < T(y) < \lambda_2) = Q_K(\sqrt{2\gamma_2}, \sqrt{\lambda_1}) - Q_K(\sqrt{2\gamma_2}, \sqrt{\lambda_2})$$
$$P(H_0|H_2) = 1 - P(H_2|H_2) - P(H_1|H_2)$$

where γ_1 is the primary SNR during data transmission, γ_2 is the primary SNR during energy transfer, and $Q_u(a, b)$ is the generalized Marcum Q-function.

In summary, the cognitive transmitter transmits data to the cognitive receiver when H_0 and H_2 are detected and harvests energy when H_1 is detected. The cognitive transmission during H_2 allows the PUs to harvest more energy, in addition to the energy from their AP. This is the purpose of the new scheme. Denote $H_p|H_q$ as one of the possible scenarios in the transmission, where H_p represents the PU status detected by the CR and H_q represents the actual PU status with $p, q = \{0, 1, 2\}$. Hence, when $p = q$, a correct detection is made. When the AP is actually transferring energy to the PUs, the received signal at the nth PU during their energy transfer is given by

$$y_n = \begin{cases} \left(h_n\sqrt{\dfrac{P_a}{L_{h_n}}}\right)x_a + \left(g_n\sqrt{\dfrac{P_s}{L_{s_n}}}\right)x_s + w_n, & H_0|H_2 \\ \left(h_n\sqrt{\dfrac{P_a}{L_{h_n}}}\right)x_a + w_n, & H_1|H_2 \\ \left(h_n\sqrt{\dfrac{P_a}{L_{h_n}}}\right)x_a + \left(g_n\sqrt{\dfrac{P_s}{L_{s_n}}}x_s\right) + w_n, & H_2|H_2 \end{cases} \tag{7.69}$$

where w_n represent the noise, P_a and P_s represent the transmitted power of the AP and the cognitive transmitter, respectively, h_n and g_n are the channel gains between AP and the nth PU and between the cognitive transmitter and the nth PU, respectively, and they are fixed during one transmission but change randomly from transmission to transmission, L_{h_n} and L_{s_n} represent the path loss between AP and the nth PU and between the cognitive transmitter and the nth PU, respectively, and x_a and x_s represent the transmitted signal by the AP and the cognitive transmitter, respectively. To explain this equation, the condition $H_0|H_2$ is the case when the AP is actually transferring energy while the CR detects it as free and hence transmits its own data to the cognitive receiver represented by the second term in the equation, $H_1|H_2$ is the case when the AP is actually transferring energy while the CR thinks that the PUs are transmitting data and hence the CR does not transmit any data, while $H_2|H_2$ is the case when the AP is actually transferring energy and this status is correctly detected by the CR so that it also sends its own data

represented by the second term in the equation to the cognitive receiver. Using y_n, the average harvested energy at each PU is derived as (Azmat et al. 2018)

$$\mathbf{E}[PE] = \eta\tau_0\left(\frac{|h_n|^2P_a}{L_{h_n}} + \frac{|g_n|^2P_s}{L_{g_n}}\right)[1 - P(H_1|H_2)] + \eta\tau_0\left(\frac{|h_n|^2P_a}{L_{h_n}}\right)P(H_1|H_2) \quad (7.70)$$

where η represents the conversion efficiency of the energy harvester.

On the other hand, the cognitive receiver receives data from the cognitive transmitter only when H_0 or H_2 are detected. Thus, the received signal at the cognitive receiver can be expressed as

$$z = \begin{cases} \left(d\sqrt{\frac{P_s}{L_d}}\right)x_s + w_d, & H_0|H_0 \\ \left(d\sqrt{\frac{P_s}{L_d}}\right)x_s + w_d, & H_2|H_0 \\ \left(d\sqrt{\frac{P_s}{L_d}}\right)x_s + \left(u_n\sqrt{\frac{P_n}{L_{u_n}}}\right)x_n + w_d, & H_0|H_1 \\ \left(d\sqrt{\frac{P_s}{L_d}}x_s\right) + \left(u_n\sqrt{\frac{P_n}{L_{u_n}}}\right)x_n + w_d, & H_2|H_1 \\ \left(d\sqrt{\frac{P_s}{L_d}}\right)x_s + \left(v\sqrt{\frac{P_a}{L_v}}\right)x_a + w_d & H_0|H_2 \\ \left(d\sqrt{\frac{P_s}{L_d}}\right)x_s + \left(v\sqrt{\frac{P_a}{L_v}}\right)x_a + w_d, & H_2|H_2 \end{cases} \quad (7.71)$$

where w_d represents the noise at the cognitive receiver with noise power $2\sigma^2$, and the channel gains and the path losses are defined accordingly. Using z, the average throughput of the CR transmission can be derived as (Azmat et al. 2018)

$$\begin{aligned} \mathbf{E}[R_{SUR}] = {} & \tau_{\text{free}}\log_2\left(1 + \frac{|d|^2P_s}{2L_d\sigma^2}\right)[1 - P(H_1|H_0)] \\ & + \tau_0\log_2\left(1 + \frac{\frac{|d|^2P_s}{L_d}}{\frac{|v|^2P_a}{L_v} + 2\sigma^2}\right)[1 - P(H_1|H_2)] \\ & + \tau_n\log_2\left(1 + \frac{\frac{|d|^2P_s}{L_d}}{\frac{|u_n|^2P_n}{L_{u_n}} + 2\sigma^2}\right)[1 - P(H_1|H_1)]. \end{aligned} \quad (7.72)$$

In the conventional energy harvesting CR, the CR operates with a different strategy. When the data transmission from the PUs to the AP is detected, the cognitive transmitter does not transmit any data. When the energy transfer from the AP to the PUs

is detected, the CR harvests energy. When no data transmission or energy transfer is detected from the PU network, the cognitive transmitter sends its own data. This is based on the traditional interweave principle that the CR must not use the licensed channel when the PU activity is detected, whether or not the PU is transmitting data or transferring energy.

In this strategy, the received signal at the nth PU becomes

$$y_n = \begin{cases} \left(h_n\sqrt{\dfrac{P_a}{L_{h_n}}}\right)x_a + \left(g_n\sqrt{\dfrac{P_s}{L_{g_n}}}\right)x_s + w_n, & H_0|H_2 \\ \left(h_n\sqrt{\dfrac{P_a}{L_{h_n}}}\right)x_a + w_n, & H_1|H_2 \\ \left(h_n\sqrt{\dfrac{P_s}{L_{h_n}}}\right)x_a + w_n, & H_2|H_2 \end{cases} \tag{7.73}$$

which gives the average harvested energy at the PU as (Azmat et al. 2018)

$$\mathbf{E}[PE] = \eta\tau_0\left(\frac{|h_n|^2P_a}{L_{h_n}} + \frac{|g_n|^2P_s}{L_{g_n}}\right)P(H_0|H_2) + \eta\tau_0\left(\frac{|h_n|^2P_a}{L_{h_n}}\right)[1 - P(H_0|H_2)]. \tag{7.74}$$

Also, the received signal at the cognitive receiver is

$$z = \begin{cases} \left(d\sqrt{\dfrac{P_s}{L_d}}\right)x_s + w_d, & H_0|H_0 \\ \left(d\sqrt{\dfrac{P_s}{L_d}}\right)x_s + \left(u_n\sqrt{\dfrac{P_n}{L_{u_n}}}\right)x_n + w_d, & H_0|H_1 \\ \left(d\sqrt{\dfrac{P_s}{L_d}}\right)x_s + \left(v\sqrt{\dfrac{P_a}{L_v}}\right)x_a + w_d, & H_0|H_2 \end{cases} \tag{7.75}$$

which gives the average throughput for the CR transmission as (Azmat et al. 2018)

$$\begin{aligned} \mathbf{E}[R_{SUR}] = {} & \tau_{\text{free}}\log_2\left(1 + \frac{\frac{|d|^2P_s}{L_d}}{2\sigma^2}\right)P(H_0|H_0) \\ & + \tau_0\log_2\left(1 + \frac{\frac{|d|^2P_s}{L_d}}{\frac{|v|^2P_a}{L_v} + 2\sigma^2}\right)P(H_0|H_2) \\ & + \tau_n\log_2\left(1 + \frac{\frac{|d|^2P_s}{L_d}}{\frac{|u_n|^2P_n}{L_{u_i}} + 2\sigma^2}\right)P(H_0|H_1) \end{aligned} \tag{7.76}$$

Next, we will compare these different strategies.

In the comparison, it is assumed that $P_s = 5.000$ dB and $\eta = 0.400$. Also, for the high channel gain case, $h_n = d = 3.000$ dB, $g_n = 2.000$ dB, $u_n = 1.300$ dB, and $v = 1.200$ dB are set, and for the low channel gain case, $h_n = 0.969$ dB, $d = 3.000$ dB, $g_n = 2.000$ dB, $u_n = 0.969$ dB, and $v = 1.200$ dB. It is also assumed that $L_{h_n} = L_d = -1.023$ dB, $L_{g_n} = -1.500$ dB, $L_{u_n} = 0.773$ dB, and $L_v = 0.569$ dB. Further, $\gamma_1 = 1.120$ dB and $\gamma_2 = 1.170$ dB

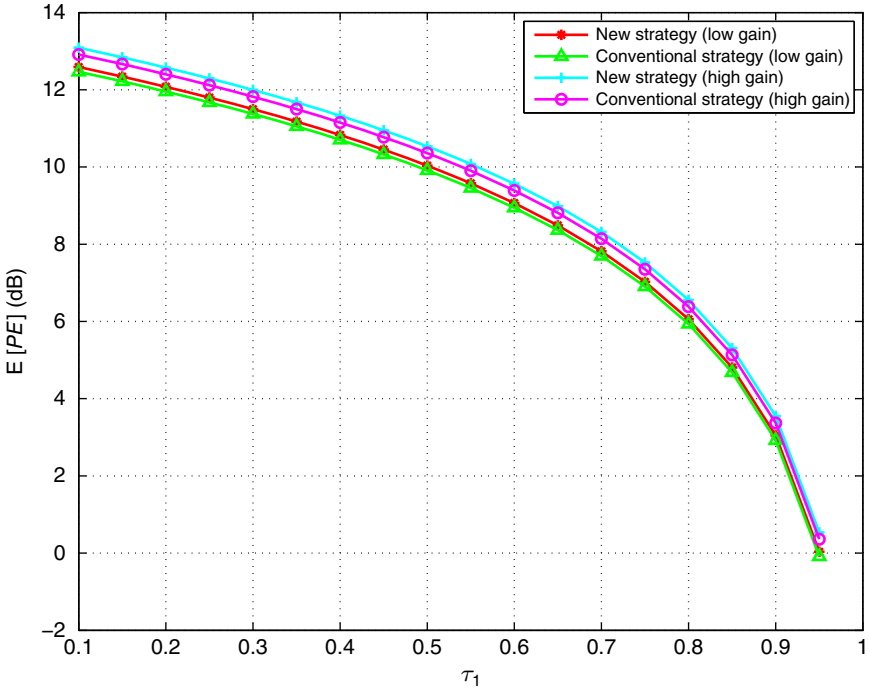

Figure 7.16 **E**[*PE*] versus τ_1.

are set, where it is assumed that SNR in H_1 is higher than that in H_2 for both strategies. Similarly, since λ_2 is larger than λ_1, we set $\lambda_1 = 5$ and $\lambda_2 = 8$.

Figures 7.16 and 7.17 show the average harvested energy at the PU and the average throughput of the CR transmission, respectively, for different values of τ_1, assuming one PU in the PU network and $T = 1$ for simplicity. One sees that the average harvested energy decreases when τ_1 increases. This is expected. When τ_1 increases, τ_0 decreases such that less energy will be harvested. The amount of harvested energy for different strategies in different cases is similar. This means the strategy and the channel gain do not change the average harvested energy much in the cases considered here. One also sees that the average throughput decreases slightly with τ_1 and then increases as τ_1 keeps increasing. When τ_1 increases, there are less chances for the CR to transmit its own data, if energy detection is correct, so that the throughput decreases. On the other hand, when τ_1 increases, τ_0 decreases so that the transmission power of the PU will be reduced due to less harvested energy. In this case, it is harder for the CR to detect its presence and hence more missed detection will occur to give the CR more transmission opportunities. From these two figures, in general, the new strategy has higher average throughput and higher average harvested energy than the conventional strategy.

In summary, the energy harvesting CR system in the previous section only harvests energy from its secondary base station so that the CR designs there only need to consider the interference temperature imposed by the PU and the wireless power is relatively stable. The energy harvesting CR system in this section harvests energy from the PU signal

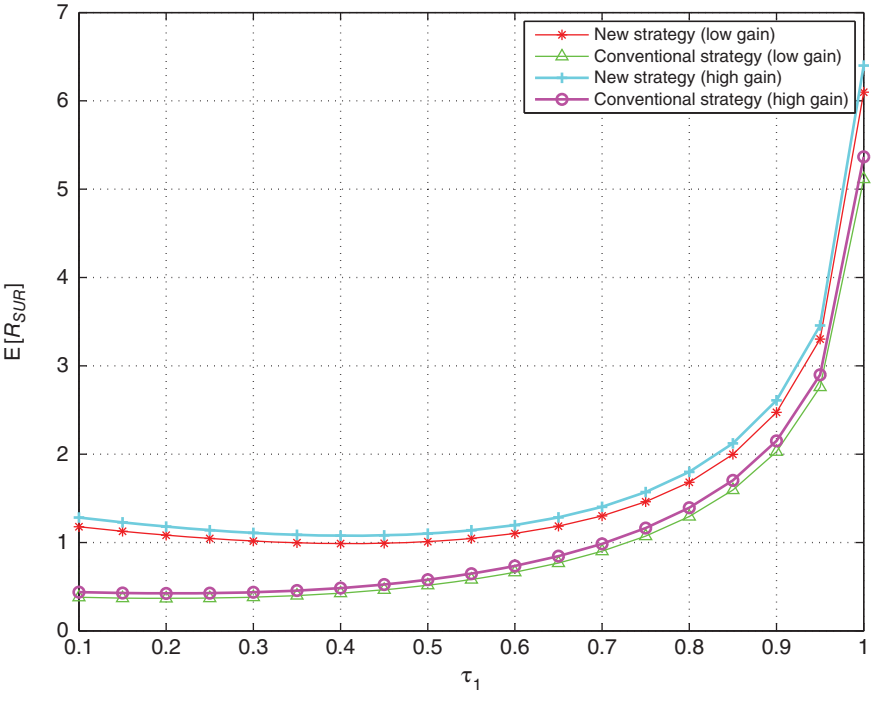

Figure 7.17 $\mathbf{E}[R_{SUR}]$ versus τ_1.

so that the CR designs need to consider both the interference temperature imposed by the PU or the unstable energy supply from the PU with random locations. Similarly, if the time-domain spectrum holes are utilized, the CR designs will need to schedule the transmission time to account for the unstable energy supply from the random traffic of the PU. This could be another line of research with many optimization problems to solve.

Next, energy harvesting CR systems that harvest energy from ambient sources will be discussed. In this case, the energy availability will be determined by the energy arrival process of the ambient source.

7.6 From the Ambient Environment

Figure 7.18 shows a diagram of the energy harvesting CR systems that harvest energy from the ambient environment. In this case, the interweave principle is considered so that spectrum sensing is necessary. The sensing accuracy will determine the collision between PU and CR, while the energy arrival rate of the ambient source will determine the energy causality. The two constraints are related to each other by the fact that, if the sensing time is long or the sensing threshold is large, a lot of energy will be consumed for spectrum sensing. This may violate the energy causality constrain due to insufficient harvested energy. However, a long sensing time or large sensing threshold may increase the sensing accuracy to reduce collision. The problem discussed in this section is to

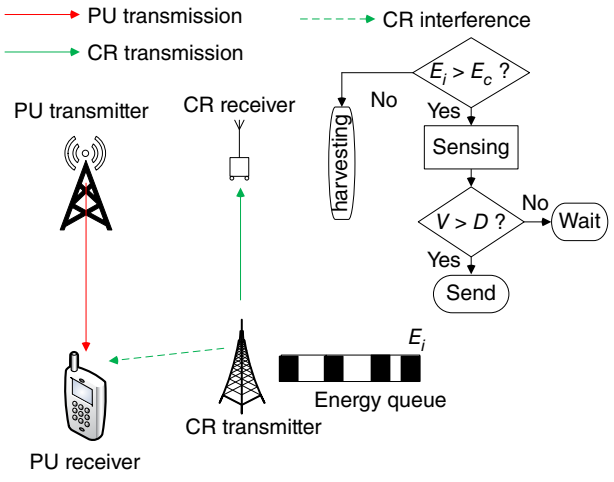

Figure 7.18 CR system that harvests energy from the ambient environment. D, detection threshold; E_c, consumed energy; E_i, incoming energy; and V, decision variable.

optimize the average throughput of the CR with respect to the sensing time and the sensing threshold, subject to the collision and energy causality constraints.

Consider the CR network where there is a pair of PU transmitter and PU receiver as well as a pair of CR transmitter and CR receiver, operating at the same location on the same frequency band. The CR network uses a slotted structure that is synchronous with the PU. The CR network assumes opportunistic spectrum access to the licensed channel, based on the sensing result and the energy availability. The licensed channel is idle with a probability of $P[H_0]$ and occupied with a probability of $P[H_1]$. The CR performs spectrum sensing in the first τ seconds and possible data transmission in the next $T - \tau$ seconds, within one time slot of T seconds. If the sensing result is correct, the CR transmission will have a throughput of $C_0 = \log_2(1 + \gamma_s)$, where γ_s is the SNR of the received CR signal. If the sensing result is incorrect, the CR transmission will suffer from the interference caused by the PU and thus have a throughput of $C_1 = \log_2(1 + \frac{\gamma_s}{1+\gamma_p})$, where γ_p is the SNR of the PU signal received at the CR receiver (Liang et al. 2008).

The energy arrival process is an important part of the system. Assume that the energy harvested during the ith time slot is E_i^h, which is an independent and identically distributed random variable with mean e_h. The actual distribution is not important, as only the mean will be used later. This is similar to the Bernoulli model discussed in Chapter 2. The battery capacity is assumed infinite so that all harvested energy can be stored and there is no energy overflow. On the energy consumption, assume that the spectrum sensing power is P_s and the data transmission power is P_b. Thus, the energy consumption of spectrum sensing is $P_s\tau$ and the energy consumption of data transmission is $P_b(1 - \tau)$. There are two decisions the CR transmitter needs to make.

First, it needs to decide whether there is enough energy to activate the sensing and transmission operations or remain idle to save energy. This is denoted by the mode indicator for the ith time slot as

$$a_i = \begin{cases} 1 & E_i \geq P_s\tau + P_b(1-\tau) \\ 0 & E_i < P_s\tau + P_b(1-\tau). \end{cases} \tag{7.77}$$

The decision is that the CR should not be activated and hence $a_i = 0$, if it is known in advance that there will not be enough energy for transmission, or vice versa. This is the energy causality constraint in the problem.

After the CR is activated, another decision that needs to be made is whether the CR should start data transmission. This depends on the spectrum sensing results for the ith time slot as

$$b_i = \begin{cases} 1 & V < D \\ 0 & V > D \end{cases} \tag{7.78}$$

where V is the decision variable and D is the detection threshold. Using the energy detector discussed in Section 7.2.2.1, one has $V = \mathbf{y}\mathbf{y}^T$. Thus, based on the Neyman–Pearson rule, the probability of false alarm is given by

$$P_f = 1 - G\left(D, \frac{K}{2}, 2\sigma^2\right) \tag{7.79}$$

and the probability of detection is given by

$$P_d = 1 - G\left[D, \frac{K}{2}, 2\sigma^2(1+\gamma_p)\right]. \tag{7.80}$$

If one assumes a sampling frequency of f_s during spectrum sensing, one has $K = \tau f_s$. Thus,

$$P_f(\tau, D) = 1 - G\left(D, \frac{\tau f_s}{2}, 2\sigma^2\right) \tag{7.81}$$

and

$$P_d(\tau, D) = 1 - G\left[D, \frac{\tau f_s}{2}, 2\sigma^2(1+\gamma_p)\right]. \tag{7.82}$$

Based on the above, the overall energy consumption during the ith time slot is given by

$$E_i^c = a_i[P_s\tau + (1-b_i)P_b(1-\tau)] \tag{7.83}$$

and thus, the residual energy for the $(i+1)$th time slot is

$$E_{i+1} = E_i + E_i^h - E_i^c. \tag{7.84}$$

The energy causality is determined by the relationship between the harvested energy E_i^h and the energy consumption E_i^c. It is difficult to consider the instantaneous energy causality, as different time slots are correlated through the residual energy in (7.84). To simplify this analysis, one could use the average energy. In this case, the energy causality constraint becomes the constraint where the average energy consumption must be smaller than the average harvested energy. One has

$$Pr[a_i = 1] \leq \min(1, \lambda(\tau, D, e_h)) \tag{7.85}$$

where

$$\lambda(\tau, D, e_h) = \frac{e_h}{P_s\tau + P_b(1-\tau)[P[H_0](1-P_f(\tau, D)) + P[H_1](1-P_d(\tau, D))]}. \tag{7.86}$$

Detailed discussions can be found in Park and Hong (2013) and Chung et al. (2014). If the CR transmitter always activates whenever there is enough energy, the equality in (7.85) will be taken and the probability of activation can be approximated as

$$P_a(\tau, D, e_h) = \min(1, \lambda(\tau, D, e_h)). \tag{7.87}$$

The value of $\lambda(\tau, D, e_h)$ actually gives the ratio of the average harvested energy to the average energy consumption. Using (7.86), three system statuses can be defined.

If $\lambda(\tau, D, e_h) > 1$, this is the energy-surplus status. In this status, the average harvested energy is always enough for sensing and transmission. This status is actually the conventional CR systems without energy harvesting.

If $\lambda(\tau, D, e_h) < 1$, this is the energy-deficit status. In this status, there might be a lack of energy such that the CR transmitter will go to the idle mode. This is a unique status for energy harvesting CR.

If $\lambda(\tau, D, e_h) = 1$, this is the energy-equilibrium status.

Using the above results, the CR will start data transmission in two cases. In the first case when the licensed channel is free, $a_i = 1$ and $b_i = 0$, the throughput is given by C_0. This happens with a probability of $P[H_0]P_a(\tau, D, e_h)(1 - P_f(\tau, D))$. In the second case when the licensed channel is occupied, $a_i = 1$ and $b_i = 0$, the throughput is given by C_1. This happens with a probability of $P[H_1]P_a(\tau, D, e_h)(1 - P_d(\tau, D))$. Thus, the average throughput is

$$\begin{aligned} R(\tau, D, e_h) = \frac{T - \tau}{T}[&C_0 P[H_0]P_a(\tau, D, e_h)(1 - P_f(\tau, D)) \\ &+ C_1 P[H_1]P_a(\tau, D, e_h)(1 - P_d(\tau, D))] \end{aligned} \tag{7.88}$$

where $T - \tau$ takes the penalty of sensing into account. This average throughput can be further approximated as

$$\begin{aligned} R(\tau, D, e_h) &\approx \frac{T - \tau}{T}[P[H_0]P_a(\tau, D, e_h)(1 - P_f(\tau, D)) \\ &\quad + P[H_1]P_a(\tau, D, e_h)(1 - P_d(\tau, D))]C_0 \\ &= \min(1, \lambda(\tau, D, e_h))\hat{R}(\tau, D) \end{aligned} \tag{7.89}$$

because when γ_p is large, $(1 - P_d(\tau, D)) \approx 0$ and when γ_p is small, $C_1 \approx C_0$. Finally, the optimization problem is

$$\max_{\tau, D} \{\min(1, \lambda(\tau, D, e_h))\hat{R}(\tau, D)\} \tag{7.90}$$

$$\min(1, \lambda(\tau, D, e_h))(1 - P_d(\tau, D)) \leq \bar{P}_c \tag{7.91}$$

where $\bar{P}_c$ is the maximum possibility of collision allowed by the PU. The solution to this problem depends on the system status.

If the system is in the energy-surplus status, one has $\lambda(\tau, D, e_h) > 1$. Thus, the optimization becomes

$$\max_{\tau, D} \{\hat{R}(\tau, D)\} \tag{7.92}$$

$$(1 - P_d(\tau, D)) \leq \bar{P}_c \tag{7.93}$$

and one has (Chung et al. 2014)

$$\tau^{opt} = \max_{\tau} \left\{ \frac{T - \tau}{T}[P[H_0](1 - P_f(\tau, D)) + P[H_1]\bar{P}_c]C_0 \right\} \tag{7.94}$$

$$D^{opt} = P_d^{-1}(\tau^{opt}, 1 - \bar{P}_c) \tag{7.95}$$

where $P_d^{-1}(\cdot)$ is the inverse function of $P_d(\cdot)$. This status only appears when $\lambda(\tau^{opt}, D^{opt}, e_h) > 1$ or $e_h > P_s\tau^{opt} + P_b T/C_0\hat{R}(\tau^{opt}, D^{opt})$. Thus, the optimum solutions

in (7.94) need to be checked against the condition on e_h. In this case, the optimum sensing time τ^{opt} is actually the same as those in Liang et al. (2008) when there is no energy harvesting.

If the system is in the energy-deficit status, $\lambda(\tau, D, e_h) < 1$ and

$$\max_{\tau,D} \{\lambda(\tau, D, e_h)\hat{R}(\tau, D)\} \tag{7.96}$$

$$\lambda(\tau, D, e_h)(1 - P_d(\tau, D)) \leq \bar{P}_c, \lambda(\tau, D, e_h) < 1. \tag{7.97}$$

There is no analytical solution but the optimum values of τ and D can be obtained from

$$\max_{\tau,D} \left\{ \min \left(1, \frac{\bar{P}_c}{1 - P_d(\tau, D)} \right) \hat{R}(\tau, D) \right\} \tag{7.98}$$

using numerical methods.

If the system is in the energy-equilibrium status, there is only one pair of optimum values obtained from

$$D^{opt} = P_d^{-1}(\tau^{opt}, 1 - \bar{P}_c) \tag{7.99}$$

$$e_h = P_s\tau^{opt} + P_b(T - \tau^{opt})[P[H_0](1 - P_f(\tau^{opt}, D^{opt})) + \bar{P}_c P[H_1]]. \tag{7.100}$$

A full derivation of these equations can be found in Chung et al. (2014).

The above designs optimize the average throughput with respect to the sensing time and the sensing threshold jointly. One can also optimize the sensing threshold alone for a fixed sensing time. This was done in Park et al. (2013) and Park and Hong (2014), where the probability of accessing an idle channel was maximized subject to a constraint on the collision probability. Also, the above design simplifies the problem by considering a fixed slot structure. The CR always accesses the spectrum when it is activated and the channel is detected free. One can also optimize the access policy so that the optimum sensing strategy can be derived (Park and Hong 2013). A joint optimization is also possible (Yin et al. 2015). Essentially, one can derive different performance measures that are of interest for different applications and optimize them with respect to different parameters in the design. For all these designs, since the energy source is independent of the PU, the energy causality and the collision constraints are separate, which has simplified the problem greatly. If the energy source is the PU signal, then sensing interval, harvesting interval, and transmission interval have to be jointly optimized so that the above designs have many variants.

Also, the above designs used energy detection. Feature detectors can also be used. In this case, different solutions to the optimization problems can be obtained (Gao et al. 2016b). Also, the battery capacity is assumed infinite. In practice, they are of finite size such that there will be extra constraints on the energy process. These results can also be extended to the case of multiple CR nodes. In this case, collaboration is possible so that a joint optimization across different nodes can be conducted (Bae and Baek 2015).

Finally, instead of using the average energy causality, one can use the instantaneous energy. In this case, the problem will be more complicated, as each time slot will be considered to design an optimum spectrum access policy. At the beginning of each time slot, one needs to make the two decisions on activation and transmission. This involves the best resource allocation in the time domain as well as online energy management (Zhang et al. 2016).

All the above results, regardless of their energy sources, have focused on either the underlay system or the interweave system. Next, the overlay system will be discussed, where energy and information become two important resources for exchange between the CR and the PU.

7.7 Information Energy Cooperation

In this case, the CR cooperates with the PU when the PU link is in outage, in exchange for the transmission opportunities in the licensed channel. This follows the overlay principle. A diagram of this system is given in Figure 7.5. To achieve this, the CR and the PU must share more information about the system via dedicated control channels.

Consider a CR network with a pair of PU transmitter and PU receiver and a pair of CR transmitter and CR receiver. All nodes have a single antenna except the CR transmitter that has N antennas. This makes beamforming possible and therefore makes the CR transmission more efficient. The communication time T is evenly divided into two parts. In the first $\frac{T}{2}$, the PU transmitter broadcasts its data. This signal will be received at the PU receiver as

$$y_{SD} = \sqrt{P_p} h s_p + n_{SD} \tag{7.101}$$

where P_p is the transmission power of the PU, h is the complex Gaussian fading gain between the PU transmitter and the PU receiver and can be considered as fixed in block-fading channels, s_p is the symbol transmitted by the PU with $E\{|s_p|^2\} = 1$, and n_{SD} is the AWGN with mean zero and variance $2\sigma^2$. Also, the same signal will be received by the CR transmitter as

$$\mathbf{r_{SR}} = \sqrt{P_p}\mathbf{h} s_p + \mathbf{n_{SR}} \tag{7.102}$$

where $\mathbf{h}$ is the fading gain vector between the PU transmitter and different antennas at the CR transmitter and $\mathbf{n_{SR}}$ is the AWGN at the CR transmitter each element of which has mean zero and variance $2\sigma_a^2$. The signal in (7.101) does not provide enough rates for the PU link and hence help from the CR transmitter is needed.

The received signal at the CR transmitter is split into two parts: one for energy harvesting; and one for information forwarding. This is similar to the PS scheme discussed in Chapter 6 for SWIPT. The signal for forwarding is given by

$$\bar{\mathbf{r}}_{\mathbf{SR}} = \sqrt{1-\rho}\mathbf{r_{SR}} + \bar{\mathbf{n}}_{\mathbf{R}} \tag{7.103}$$

where ρ is the power splitting factor, as discussed in Chapter 6, and $\bar{\mathbf{n}_{\mathbf{R}}}$ is the AWGN during the signal processing after the splitting with mean zero and variance $2\sigma_d^2$. One has $2\sigma^2 = 2\sigma_a^2 + 2\sigma_d^2$. The other part $\sqrt{\rho}\mathbf{r_{SR}}$ is used for energy harvesting to give the harvested energy

$$E_h = \frac{T}{2}\eta\rho P_p ||\mathbf{h}||^2 \tag{7.104}$$

where η is the conversion efficiency and $||\mathbf{h}||^2$ is the total energy harvested from the PU. As before, the noise energy is ignored, as it is negligible compared with the signal energy. If the CR transmitter has an initial power of P_s, the total power or the maximum power

available at the CR transmitter becomes $P_{max} = P_s + \eta\rho P_p||\mathbf{h}||^2$, since the transmission time in the second half is also $\frac{T}{2}$.

The CR transmitter combines its own signal and the PU signal via superposition as

$$\mathbf{x} = \mathbf{w}_s s_s + \mathbf{w}_p \mathbf{h}^H \bar{\mathbf{r}}_{\mathbf{SR}} \tag{7.105}$$

where $\mathbf{w}_s$ is the beamforming vector for its own data s_s with $E\{|s_s|^2\} = 1$, $\mathbf{w}_p$ is the beamforming vector for the PU data, and $(\cdot)^H$ represents the conjugate transpose operation. This signal is transmitted in the second half of T. During this transmission, the PU transmitter remains silent. This is only possible when there is cooperation between CR and PU to avoid interference.

Thus, the received signal at the CR receiver is

$$r_{RR} = \mathbf{g}^H \mathbf{x} + n_{RR} \tag{7.106}$$

where $\mathbf{g}$ is the fading gain vector from different antennas at the CR transmitter to the CR receiver, and n_{RR} is the AWGN at the CR receiver with mean zero and variance $2\sigma^2$. The received signal at the PU receiver is

$$y_{RD} = \mathbf{f}^H \mathbf{x} + n_{RD} \tag{7.107}$$

where $\mathbf{f}$ is the fading gain vector from different antennas at the CR transmitter to the CR receiver, and n_{RD} is the AWGN at the PU receiver with mean zero and variance $2\sigma^2$. From (7.106), the SNR at the CR receiver is

$$\Gamma_s = \frac{|\mathbf{g}^H \mathbf{w}_s|^2}{|\mathbf{g}^H \mathbf{w}_p|^2 ||\mathbf{h}||^2 [(1-\rho)P_p ||\mathbf{h}||^2 + (1-\rho)2\sigma_a^2 + 2\sigma_d^2] + 2\sigma^2}. \tag{7.108}$$

Thus, the achievable rate for the CR link is

$$R_s = \log_2(1 + \Gamma_s). \tag{7.109}$$

Also, from (7.107), the SNR at the PU receiver is

$$\Gamma_p = \frac{\rho P_p ||\mathbf{h}||^4 |\mathbf{f}^H \mathbf{w}_p|^2}{|\mathbf{f}^H \mathbf{w}_s|^2 + |\mathbf{f}^H \mathbf{w}_p|^2 ||\mathbf{h}||^2 [2\sigma_d^2 + (1-\rho)2\sigma_a^2] + 2\sigma^2}. \tag{7.110}$$

Thus, the achievable rate for the PU link is

$$R_p = \frac{1}{2}\log_2\left(1 + \frac{P_p |h|^2}{2\sigma^2} + \Gamma_p\right) \tag{7.111}$$

where maximum ratio combining is used to combine the signals from the CR transmitter and the PU transmitter. Thus, for this energy harvesting CR system, the optimization problem is

$$\max_{\mathbf{w}_s, \mathbf{w}_p, \rho} \{R_s\} \tag{7.112}$$

$$R_p \geq r_0 \tag{7.113}$$

$$E\{||\mathbf{x}||^2\} \leq P_{max} \tag{7.114}$$

$$0 \leq \rho \leq 1. \tag{7.115}$$

where

$$E\{||\mathbf{x}||^2\} = ||\mathbf{w}_s||^2 + ||\mathbf{w}_p||^2||\mathbf{h}||^2[P_p(1-\rho)||\mathbf{h}||^2 + (1-\rho)2\sigma_a^2 + 2\sigma_d^2] \quad (7.116)$$

and r_0 is the minimum rate that is required by the PU. More details on the above equations can be found in Zheng et al. (2014).

This optimization problem does not have a closed-form solution in the general case. However, two special cases can be discussed. First, if zero-forcing is used for beamforming, one has $\mathbf{w}_p = \sqrt{\omega_p}\frac{(\mathbf{I}-\frac{\mathbf{gg}^H}{||\mathbf{g}||^2})\mathbf{f}}{||(\mathbf{I}-\frac{\mathbf{gg}^H}{||\mathbf{g}||^2})\mathbf{f}||}$ and $\mathbf{w}_s = \sqrt{\omega_s}\frac{(\mathbf{I}-\frac{\mathbf{ff}^H}{||\mathbf{f}||^2})\mathbf{g}}{||(\mathbf{I}-\frac{\mathbf{ff}^H}{||\mathbf{f}||^2})\mathbf{g}||}$. In this case, closed-form expressions for the optimal solutions are available. Secondly, if the CR transmitter only has one antenna, no beamforming is needed. In this case, the optimization will be much simpler. The above results use power splitting. One can also use time switching to obtain a similar optimization problem. Details can be found in Zheng et al. (2014).

Note that this energy harvesting CR system is very similar to the energy harvesting relaying to be discussed in Chapter 8 as it uses the overlay principle. The main difference is that, in Chapter 8, the relay only forwards the signal received from the source, while here the CR combines its own signal with the PU signal before forwarding. This superposition comes at a price, for example, increased peak-to-average-power ratio.

The above results also have many other variants. For example, in Zhai et al. (2016b), a similar cooperative strategy was considered between CR and PU for more complicated cases, such as the Alamouti space-time coding. In Hsieh et al. (2016), the CR becomes the node with fixed power supply, while the PU harvests energy from the CR transmission if it does not have enough energy. In this case, the precoding matrix at the CR and the energy harvesting parameter at the PU have been jointly optimized to maximize the CR information rate, while satisfying the minimum required rate and the harvested energy at the PU. In Zhai et al. (2016a), the PU uses wireless power, while the CR has a fixed power supply. The CR close to the PU power transmitter is chosen to relay the energy to the remote PU node. Finally, in Yin et al. (2014), the optimal cooperation strategy for the CR was studied. In this case, the CR can choose to cooperate with the PU if it has enough energy for its own data transmission but otherwise can wait until the PU finishes transmission.

In many of these studies, energy harvesting is performed by the PU, not the CR, and the PU trades the transmission opportunity for energy from the CR. In other studies, the CR helps the PU with its information delivery in exchange for the transmission opportunity.

7.8 Other Important Issues

The previous sections have mainly discussed the effect of different energy sources on the designs of energy harvesting CR systems. In these sections, optimization problems have been formulated that maximize the achievable rate of the CR subject to constraints from energy causality and/or collision with the PU. These optimizations focus on the choice of the transmission power for CR data transmission and the sensing interval and threshold for CR spectrum sensing. In addition to these designs, other important issues in energy harvesting CR have also been looked into.

For example, the secrecy performance is very important in wireless communications due to the broadcast nature of the wireless media. In Singh et al. (2016), the secrecy outage of the cognitive HAP wireless powered system was analyzed. The difference between this analysis and the conventional HAP system is that the transmission power of Alice as a CR node needs to be limited by the interference temperature imposed by the PU. In Jiang et al. (2016), the information rate of the CR node was optimized with respect to the beamforming vector for the CR node, the beamforming vector for the PU and the power splitting factor, with a constraint on the minimum secrecy rate required by the PU and another constraint on the minimum SINR required by the PU. In Ng et al. (2016), artificial noise was generated and optimized to achieve the best energy harvesting efficiency or transmission power.

Channel selection is another important issue in CR communications. It is often the case in practice that there will be more than one licensed channel available to the CRs. From the data transmission point of view, the CR should choose a channel with as little PU traffic as possible to make use of the transmission opportunities. However, from the energy harvesting point of view, the CR should choose a channel with as much PU traffic as possible so that it can harvest the maximum amount of energy from the PU. For a CR node that performs both data transmission and energy harvesting, a tradeoff has to be made. In Pratibha et al. (2016), this tradeoff was studied to maximize the average information rate of the CR, averaged over different PU channels, using the same system model as Lee et al. (2013). Depending on the density of the CR nodes, there could be a significant rate increase compared with the scheme that chooses channels uniformly or equally. This work assumes that the CR harvests energy from the PU. On the other hand, if the CR harvests from the ambient source, as in Pradha et al. (2014), the effect of the energy availability on channel selection can be analyzed and then the channel selection policy can be optimized based on the amount of available harvested energy.

There are other important issues in CRs, such as spectrum handover, spectrum aggregation, and spectrum allocation. They can be studied in a similar way by considering the dynamics of the energy supply for energy harvesting CR.

7.9 Summary

Energy harvesting can be combined with CRs to provide energy- and spectral-efficient wireless communications. This chapter has discussed different energy harvesting CR systems. The discussion has been based on the source of energy for the CR, as the source of energy makes a fundamental difference to the CR design. Several important energy harvesting CR systems have been investigated, where the CR system is a wireless powered communications system, the CR harvests energy from the PU signal, or the CR harvests energy from random ambient sources. Within these systems, different spectrum sharing principles have been examined. For interweave systems, spectrum sensing is required and the interference on the PU is determined by the sensing accuracy. Different sensing methods have different sensing accuracies. For underlay systems, an interference temperature will be in place. For overlay systems, it resembles the energy harvesting cooperative communications system to be discussed later.

The design problems in these systems often involve an optimization, where the objective function could be information rate, the amount of harvested energy, or other performance measures, while the constraints mainly come from the energy causality that the harvested energy must be larger than the energy to be consumed and the collision that the PU must be protected from. Then, either numerical methods or standard optimization methods can be applied to solve these problems. Following this idea, if a previous study is in the CR literature, one needs to add the energy causality constraint or consider the dynamics of the energy supply, while if a previous study is in the energy harvesting literature, one needs to add the collision constraint. In some cases, both constraints need to be considered.